IMPACT PROOF PRELIMINARY DESIGN FOR THE

MARINE BIOLOGY STATION IN DICHATO

2016/2017

PART II

DESIGN

Contents

LIST OF FIGURES

LIST OF TABLES

5 DESIGN PROCESS

Part II: Design presents the design of all relevant elements of the Marine Biology Station as determined in the problem analysis. These elements include 1) a jetty according to the 'Traditional' option presented in Part I: Analysis; 2) a breakwater, also corresponding to the 'Traditional' option; 3) the deteriorated EMBD building which requires reconfiguration; and 4) pavement connecting the jetty to the infrastructure of Dichato.

The onshore structures are not the focus of this project; thus they are not developed past the rule-of-thumb stage. The jetty and the breakwater, on the other hand, are designed in phases, moving from dimensioning to a more detailed design. Iterations are carried out to adjust dimensions so as to avoid under- or over dimensioning. The scope, however, of the overall design which is presented for the Marine Biology Station, is limited to a *preliminary* design. A definitive design will require further iteration and detailing of connections and installations. Figure 5-1 illustrates the design process which is adopted.

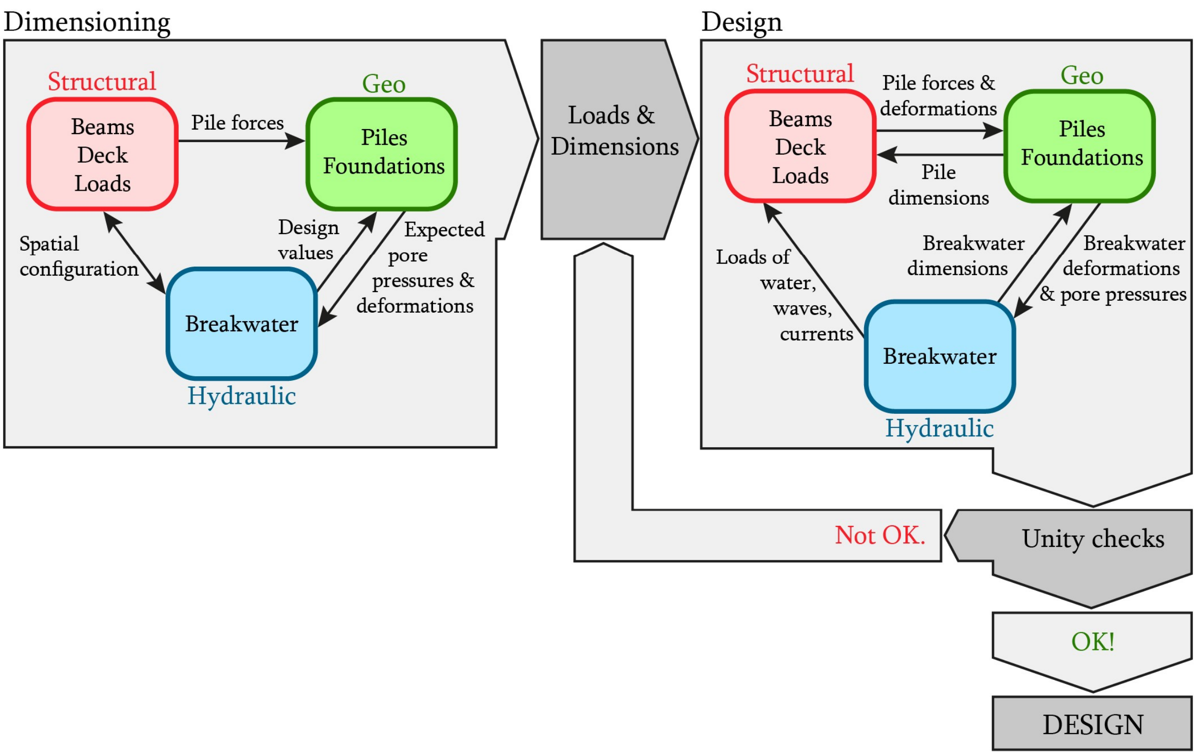

Figure 5-1: Flow diagram for jetty and breakwater design process

6 PRELIMINARY DESIGN: JETTY

For the dimensioning of the jetty and its foundation piles, consult Appendix E.

6.1 DESIGN APPROACH

According to the traditional design, as can be seen in the reference project in Coliumo (Appendix C), a steel-concrete structural design will be made consisting of:

- Round and hollow steel piles;
- Steel H-beams and;
- Concrete deck, cast in-situ.

Professor of Strcutural Mechanics of UdeC, Dr. Dechent, presented several configurations during his lecture of December 1, 2016. The three configurations that will be looked at in more detail in Chapter 6.1.1.

The first step in the structural design approach is to estimate the configuration and dimensioning of all structural element using rules of thumb.

Secondly, all load cases and load combinations will be defined apart from the earthquake actions, using multiple Chilean building standards. When all input has been determined, a model will be constructed with CSI software ETABS (ETABS, 2016). This program derives the self-weight and the fundamental period needed to calculate the seismic load.

The following step is to apply all the load combinations, including seismic loads, in the program ETABS and to derive the pile forces that can be used for the foundation design. After estimating the minimum required pile dimensions, unity checks can be performed for all structural elements. Based on these unity checks, it can be found out whether elements are over or under dimensioned. When it is decided to change element dimension, it is necessary to redo the unity checks.

6.1.1. CONFIGURATIONS

So, the basic idea of the jetty design exists of a reinforced concrete deck placed on steel piles. Some of these piles need to be placed under an angle so horizontal forces acting on the jetty can be transferred to the soil. Three different configurations will be further investigated, as were presented to us by Prof. Dechent during his lecture on earthquake design of December 6, 2016. These three configurations are called Marco Duplas, Marco Flexural, and Marco Aislado. The basic designs of these configurations are illustrated in Figure 6-1.

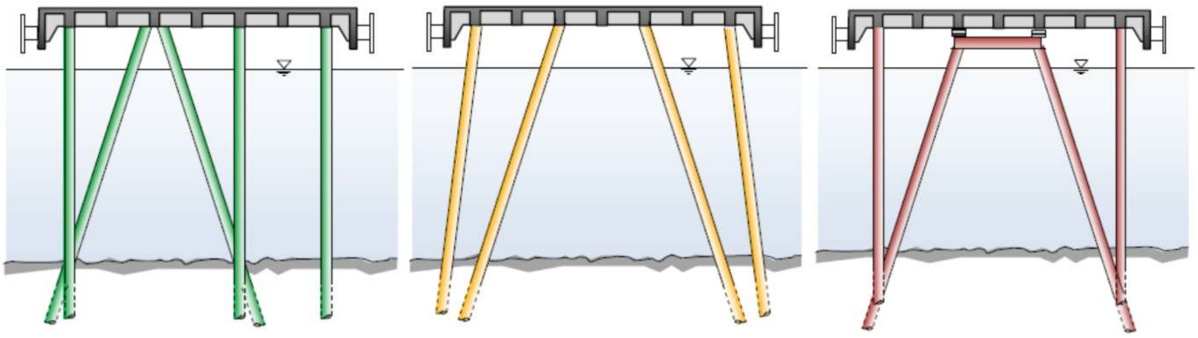

Figure 6-1: Three configurations [source: lecture Prof. Dechent]

(a) Marco Duplas *(b) Marco Flexural* *(c) Marco Aislado*

The first configuration is the Marco Duplas. The basic principle of this configuration is the use of pairs of inclined piles where necessary. Figure 6-2 shows this configuration applied to the jetty.

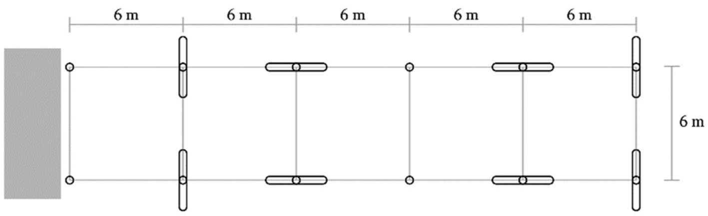

Figure 6-2: Macro Duplas

The second configuration is very similar to the first one. However, the difference consists of the use of singular inclined piles instead of the pairs of inclined piles. The structure becomes more ductile and dissipate some of the seismic energy it may be exposed to. Figure 6-3 shows this configuration applied to the jetty.

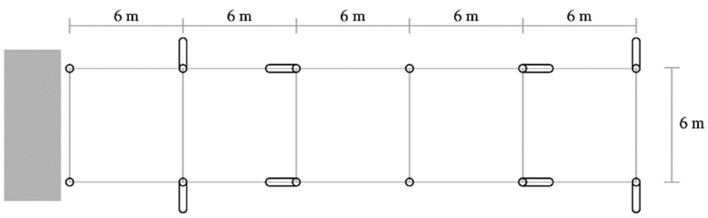

Figure 6-3: Macro Flexural

The third and last configuration which will be researched further, is a relatively new system that is being applied more and more all over Chile. In this system, an additional rigid frame has to be applied on top of the piles. The isolator will then be placed in between this rigid frame and the steel beam framework. In service conditions, the isolator acts as a bearing whereas in seismic conditions, most of the displacement will be concentrated in the isolation layer. The structure will "sway" more softly compared to the non-isolated structure. The structural damage will be minimized and the operation of the structure can be continued even during and right after the seismic event (Canam Group, 2016). Figure 6-4 shows this configuration applied to the jetty.

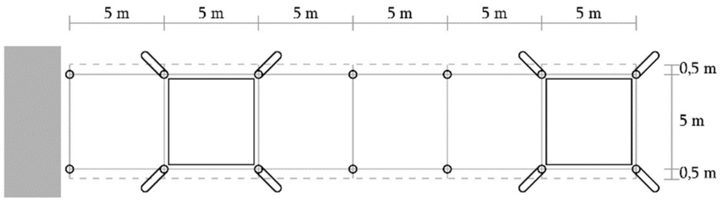

Figure 6-4: Marco Aislado

6.2 Structural Design

6.2.1 Structural Configuration

Three structural configurations are considered: Marco Duplas, Marco Flexural, and Marco Aislado.

Unfortunately, the last configuration will not be an option because for this type of jetty the isolators will not act in an effective way. A more comprehensive explanation can be found in Appendix G.1 (Bustos, 2016). After excluding the Marco Aislado configuration, models are created for Marco Duplas and Marco Flexural using software ETABS (ETABS, 2016). After researching the two different configurations, the following things emerged:

- The fundamental period of the Marco Duplas and the Marco Flexural configuration is 0.23 and 1.35 seconds, respectively.
- As mentioned before, the fundamental period is dependent on the stiffness and the mass of the system. Because the mass of the structure is small, the stiffness should be small too in order to achieve this relatively high fundamental period. The low stiffness results in too high deformations compared to the size of the jetty.
  In Chilean construction practice periods of less than 0.5 seconds are commonly recommended for this type of structure.
- The stairs are positioned outside the structure, whereby they are exposed to high (impact) loads from, for example, the vessel.
- The inclined piles are sticking out of the concrete deck, whereby they are directly subjected to high (impact) loads too.

For these reasons and after deliberation with UDEC professors, it is decided to come with an adjusted design for the jetty which overcomes the previously mentioned "problems".

The adjusted design includes a third row of steel piles which are located in longitudinal direction, in between the two existing rows of piles. First of all, this row of piles will increase the stiffness of the structure. Secondly, the middle row of piles provides the possibility of placing the inclined piles in this row so they will not stick out of the concrete deck anymore. The number and configuration of the inclined piles is extensively analysed using software ETABS (ETABS, 2016) to find an appropriate fundamental period in both x- and y-direction. As described in paragraph 6.1.1.1, this period should be lower than 0.5 seconds. The final configuration of the jetty is displayed in Figure 6-5.

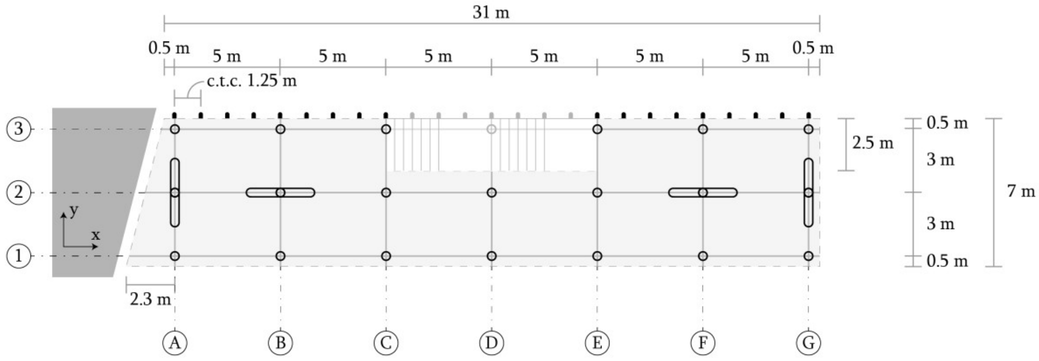

Figure 6-5: Definitive structural configuration

As can be seen from Figure 6-5, the stairs are now situated inside the concrete deck. As a result, a framework can easily be created in front of the stairs which will partly protect the stairs from being exposed to high (impact) loads. The frame exists of two longitudinal beams which will be attached to the piles on which rubber defenders are fixed (Sandoval Munoz, 2010). By applying these rubber defenders, the impact load from the vessel can be reduced.

Further, bollards can easily be placed on the concrete deck so loads on the bollards can directly be transferred to the piles underneath them.

Lastly, a triangular shaped part is added at the left-hand side of the concrete deck. This part is necessary to guarantee a good connection between the jetty and the concrete abutment.

6.2.2 Material properties

From the dimensioning in Appendix E.1, it becomes clear that two main types of materials are being used for the design of the jetty, namely reinforced concrete and steel. The reinforced concrete is made of concrete class H30 and reinforcement class A63-42H. The steel is made of steel class A36. For more details about the materials used, see Appendix G.2.

6.2.3 First step: dimensioning

As a starting point, the different structural elements, which include the deck, the piles, and the beams, need to be dimensioned following the rules of thumb. (TU Eindhoven, n.d.) The frame of the stairs is created using a steel tube profile, namely 200x150x26. The defender beams are made of steel profile H250x200x59.64 (Sandoval Munoz, 2010). An overview of the dimensions for the different elements is provided in Table 6-1. For more detail, please refer to Appendix G.3.

Table 6-1: Dimensions of structural elements

Element	Properties	
Reinforced concrete deck	Thickness, t = 250 mm	
Steel beams	H-profile	H300x300x105.5
Steel piles	Round tube profile	Ø262, t = 6 mm
Steel frame stairs	Rectangular tube profile	200x150x26
Steel defender beams	H-profile	H250x200x59.64

6.2.4 LOAD CASES

For the individual load cases, a distinction is made between loads acting from the land side, loads of and on the jetty itself and loads acting from the sea side. The loads that need to be considered are, together with their magnitude, summarized in Figure 6-6. In Appendix G.4, all loads are analysed and calculated separately. The configuration of all the loads are displayed in Figure 6-7 and Figure 6-8, the former includes all the permanent load cases and the latter includes all the live load cases.

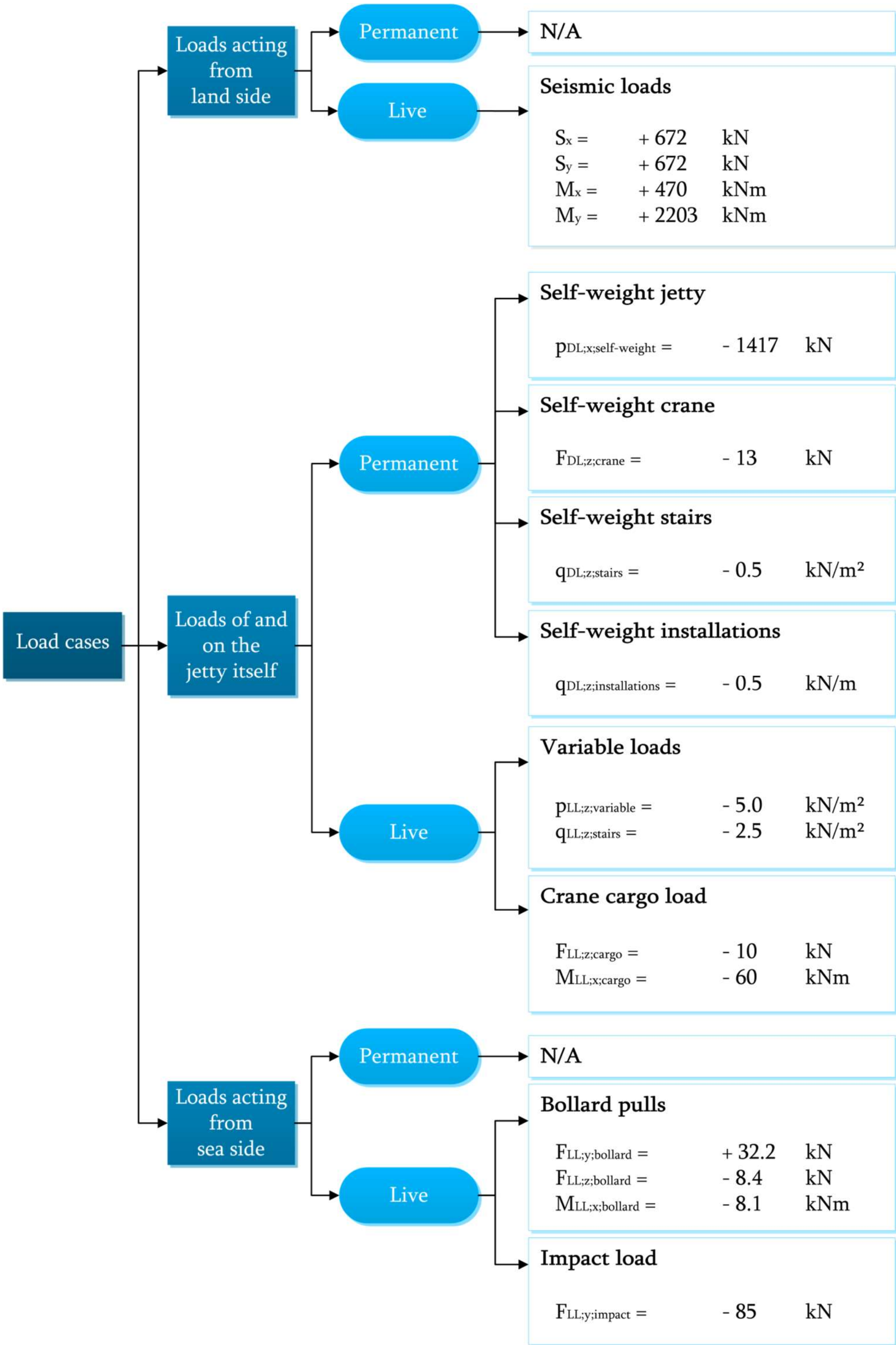

Figure 6-6: Individual load cases

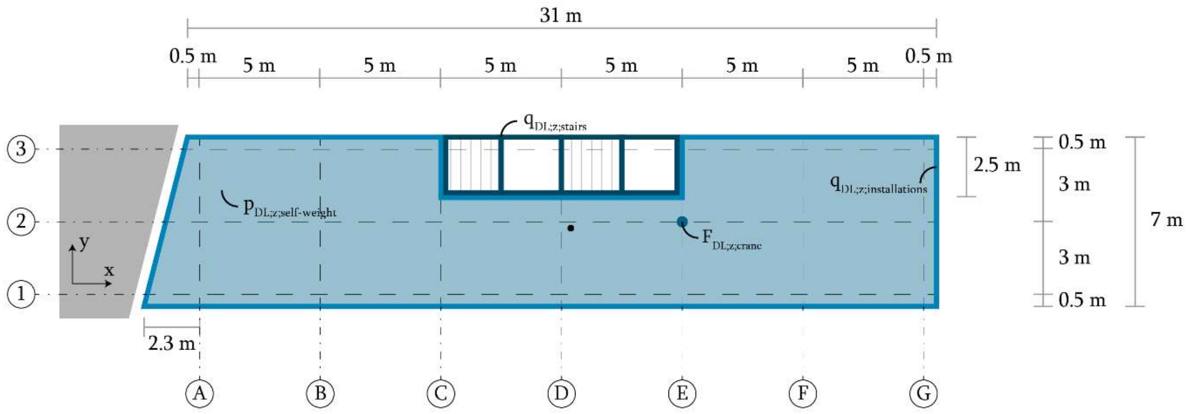

Figure 6-7: Configuration permanent loads

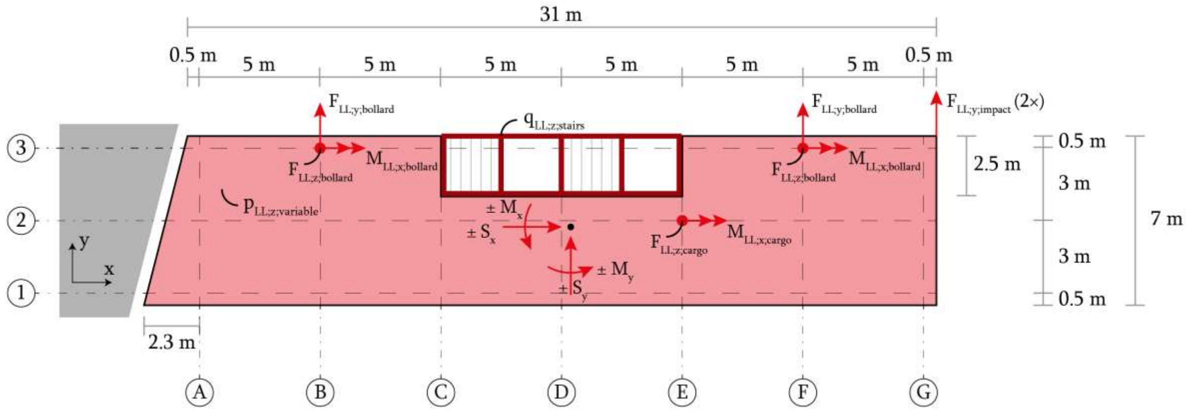

Figure 6-8: Configuration live loads

6.2.5 LOAD COMBINATIONS

For the analysis, different load combinations have to be considered. Before determining the different load combinations, general load cases are defined as in Table 6-2. Wind loads are not mentioned. The load combinations will only contain seismic based load combinations. The reason for eliminating wind load combinations is because the wind loads are relatively small compared to the seismic loads, so they will never govern the seismic load combinations.

In Chilean design, two approaches are commonly used, namely the Allowable Stress Design (ASD) and the Load and Resistance Factor Design (LRFD). The ASD combinations are based on both the code Nch2369.Of2003 (Hidalgo, 2003) and the Bachelor Thesis of S. Munoz (2010). The emerged general combinations are described in Table 6-3 and are applicable to the design of the steel structure.

Table 6-2: General load cases

Load case	D	L	B	I_1	I_2	S_x	S_y	M_x	M_y
S_x									
S_y									
M_x									
M_y									
$p_{DL;x;self\text{-}weight}$									
$F_{DL;z;crane}$									
$q_{DL;z;stairs}$									
$q_{DL;z;installations}$									
$p_{LL;z;variable}$									
$q_{LL;z;stairs}$									
$F_{LL;z;cargo}$									
$M_{LL;x;cargo}$									
$F_{LL;y;bollard}$									
$F_{LL;z;bollard}$									
$M_{LL;x;bollard}$									
$F_{LL;y;impact}$									

Table 6-3: General load combinations applicable to steel structure

	D	L	B	I_1	I_2	S_x	S_y	M_x	M_y
CS1	1								
CS2/1	1	1							
CS2/2	1	0.5	1						
CS2/3	1	0.5		1					
CS2/4	1	0.5			1				
CS3/1	1	0.5				1		1	
CS3/2	1	0.5				1		-1	
CS3/3	1	0.5				-1		1	
CS3/4	1	0.5				-1		-1	
CS3/5	1	0.5					1		1
CS3/6	1	0.5					1		-1
CS3/7	1	0.5					-1		1
CS3/8	1	0.5					-1		-1
CS4/1	1					1		1	
CS4/2	1					1		-1	
CS4/3	1					-1		1	
CS4/4	1					-1		-1	
CS4/5	1						1		1
CS4/6	1						1		-1
CS4/7	1						-1		1
CS4/8	1						-1		-1

The LRFD load combinations are based on the code Nch3171.Of2010 (Hidalgo, 2010) and are used for the design of the concrete elements, which in this case only includes the concrete deck. The load combinations are defined in Table 6-4.

Table 6-4: Load combinations applicable to concrete elements

	D	L	B	I_1	I_2	S_x	S_y	M_x	M_y
CC1	1.4								
CC2/1	1.2	1.6							
CC3/1	1.2	1				1.4		1.4	
CC3/2	1.2	1				1.4		-1.4	
CC3/3	1.2	1				-1.4		1.4	
CC3/4	1.2	1				-1.4		-1.4	
CC3/5	1.2	1					1.4		1.4
CC3/6	1.2	1					1.4		-1.4
CC3/7	1.2	1					-1.4		1.4
CC3/8	1.2	1					-1.4		-1.4
CC4/1	0.9					1.4		1.4	
CC4/2	0.9					1.4		-1.4	
CC4/3	0.9					-1.4		1.4	
CC4/4	0.9					-1.4		-1.4	
CC4/5	0.9						1.4		1.4
CC4/6	0.9						1.4		-1.4
CC4/7	0.9						-1.4		1.4
CC4/8	0.9						-1.4		-1.4

6.2.6 FINAL DESIGN: FOUNDATIONS

In the pile-dimensioning phase, the piles are tested for resistance to vertical and horizontal loads and for pull-out, following the AASHTO Geotechnical Bridge Design Manual most often used in Chile -which lacks a national geotechnical design code (AASHTO, 1998). This dimensioning is included in Appendix E.2. Following the dimensioning phase, Table 6-5 shows the pile dimensions required for structural soundness. However, the design is enhanced by considering construction aspects and failure mechanisms of the foundation elements.

Table 6-5: Foundation dimensioning results

Pile type	Batter angle	No. of piles	D x t (mm)	Pile length (m)	Profile weight (kg/m)	Axial bearing capacity (kN)
Vertical piles	-	17	262 x 6	6	37.88	550
Inclined piles	20	8 (4x2)	362 x 6	6.4	52.68	1050

6.2.6.1 Construction considerations

Pile driving equipment

In Chile, it is common practice to measure the resistance of the soil or rock during the driving process. A certain level of pile driving distance per blow in mm/blow, is predetermined as the point of 'rejection', where satisfactory bearing capacity has been reached. This method reflects the practical approach of Chilean construction practice and highlights the extent of unknown subsurface variability due to complex geology.

The steel pipes for the jetty are driven into the rock using a DELMAG D-12 diesel hammer, a commonly used rig in construction across Chile. The characteristics of this machine are given in Table 6-6, together with the calculated value for the number of blows per inch at the rejection point, N_b. At this point of embedment, the pile has developed sufficient bearing capacity. Considering the harbour application, the piles must be driven from a floating pontoon. Appendix G.6.1 gives a full computation of N_b.

Table 6-6: Characteristics of DELMAG D-12 pile driving rig, [source: www.hammersteel.com]

Energy per blow	[kg m]	3125
Piston weight	[kg]	1250
N_b	[mm / blow]	32.3 (vertical pile) 13.0 (inclined pile)

Pile buckling during driving

The governing load situation for buckling of the steel pile is during pile driving. In Chile, the American code AISC 360-05 *Specification for Structural Steel Buildings* is used to assess this phenomenon (ANSI, 2005). Appendix G.6.2 gives the corresponding determination of the ultimate compressional strength of the governing pile during pile driving, as well as a check on slenderness. Both conditions are satisfied.

Anchoring

From the dimensioning phase, the pull-out capacity of the inclined piles subject to tension emerged as insufficient. To retain the slender design, measures must be taken to resist pull-out. Since it is not possible to embed the piles beyond 2m into the rock, it is necessary to anchor them. As it is assumed that the inclined piles resist all tensional loads, it is not necessary to anchor the vertical piles.

A possible method to achieve anchoring is to drill ahead into the rock a long socket of slightly smaller diameter than the inside diameter of the pile, followed by the insertion of a pile into the socket with grout pipes attached it. It is then grouted up, bonding the insert pile to the walls of the socketed hole and primary pile above (Srinivasamurthy & Pujar, 2009). This is based on a micropiling system as illustrated in Figure G-17 in Appendix G.6.2, and is commonly applied in Chile. A recent local application is a jetty built in the nearby Puerto Lirquén. The piles of this jetty are set is metamorphic rock which was impossible to penetrate deep enough to develop sufficient uplift capacity.

Corrosion

Appendix G.6.2 gives background information on steel corrosion in marine environments. For the jetty to be constructed in Dichato, the most suitable option is sacrificial anode cathodic protection, since applying a protective coating would require regular maintenance, which is often not carried out sufficiently in Chilean port works. The other form of cathodic protection, Impressed Current Cathodic Protection, is uneconomical for small jetties. The sacrificial anodes usually have a protective limit of 5-7m of pile length and a lifetime of 10 years (PDCA, 2001). It is suggested to apply this protection method in combination with the previously determined 4mm of added steel thickness.

6.2.6.2 Failure mechanisms

Besides uplift and buckling, the foundation piles of the jetty may be subjected to the following two general failure mechanisms: 1) (differential) settlement 2) liquefaction-induced failures and 3) scour.

Deformation and settlement

For a distance of 5 m between foundation elements, the following deformation restrictions apply for geotechnical structures according to the Dutch geotechnical code for *Basic requirements and loads* (NNI, 2006). The settlement for the point-bearing piles are computed in Appendix G.6.2, and the results are presented in Table 6-8 for both the heaviest and lightest loaded piles.

Table 6-7: Deformation requirements for geotechnical structures

	ULS	SLS
Pile foundation settlement W, m	0.15	0.05
Structure[1] settlement W, m	-	0.15
Structure relative rotation β	1:100	1:300

Table 6-8: Ultimate pile settlements for vertical piles

		Smallest vertical pile load	Largest vertical pile load
P	kN	34.6 (pile C19)	192.0 (pile C49)
S_0	m	0.0026	0.014

The majority of the settlement (90%) is due to the settlement of the soft sandstone, whereas the elastic compression of the pile S_e is minimal. Overall, the individual settlements are well within the accepted boundaries as in. In terms of differential settlement, the rotation due to differences in settlements over a lateral pile distance of 6m would be 0.109° or 1:500. Considering that this simplification disregards pile group effects and the presence of the raked piles, the settlements and resulting rotation are acceptable.

The settlement of a group of point bearing piles corresponds to the settlement of individual piles if the piles are resting on rock. Differential settlements are unlikely to occur as all piles are embedded in the sandstone at an equal depth. However, in general, assessing the settlement of point bearing

[1] Refers to residential building. Values for harbour facilities are unknown.

piles is inaccurate without test loadings; static test loadings should be performed to observe the settlement of the pile point (Tol, 2006). The settlement analysis has been conducted only on the vertical piles, as it is assumed that the majority of the vertical loads is resisted by the vertical piles. However, the presence of raked piles generally improves the settlement performance besides obvious improvement in lateral deflections and cap rotation. On the other hand, raked piles may negatively affect the deformation performance in the presence of horizontal or vertical ground movements due to bending moments induced in the piles (Poulos, 2006).

Liquefaction and lateral spreading

In the case of the jetty foundation, liquefaction induced by seismic activity may cause uncontrolled or differential settlement and temporary loss of bearing capacity. These failure mechanisms for single piles in liquefied layers are demonstrated in Appendix G.6.

To investigate the risk of any of these mechanisms to affect the stability of the jetty and its foundation, a liquefaction potential (*LP*) analysis of the soil is carried out (Youd, Idriss, Andrus, & Arango, 2001). The *LP of* a soil is defined as the ratio between the Cyclic Resistance Ratio CRR (the capacity of the soil to resist liquefaction) and the Cyclic Stress Ratio CSR (the seismic demand on a soil layer). A commonly used safety factor worldwide for this susceptibility ratio is 1.2. The computation of both the CRR and CSR are given in Appendix G.6.2, as well as the corresponding data tables.

Figure 6-9 shows a depth profile of SPT blow count corresponding to Appendix B.4 boreholes. Since the soil profile varies between the proposed start and end of the jetty, the boreholes at these two extreme locations are used in the analysis, S6 and S3, respectively. The grey line in Figure 6-9 gives the predicted SPT profile if the soft soils lying atop the sedimentary rock were to be excavated to a level of MSL -2.5m.

Figure 6-10 gives the results of the liquefaction analysis, see Appendix G.6.2 for the method of computation of the liquefaction potential, LP. The full lines indicate the LP values at the start and end of the jetty, as well as for the whole jetty after excavation. The dotted lines indicate the required LP value with depth for a factor of safety of 1.2. At the start of the jetty the soft soil (silt, ML) is highly liquefaction susceptible with a LP value of less than 0.2. The first two meters of soil (silty sand, SM) near the end of the jetty, are also susceptible to liquefaction If the soil were to be excavated to a level of MSL -2.5m along the entire length of the proposed jetty location, the liquefaction potential criterion of 1.2 would always be satisfied (for corrected N values $(N_1)_{60}$ of greater than 30, the soil is considered too dense to liquefy). [2]

[2] 1.2 (required F.O.S.) is taken as the maximum possible Liquefaction Potential value in Figure 6-10

Overall it may be concluded that it is indeed necessary to excavate to MSL -2.5m, as the soil lying atop the sedimentary rock is highly susceptible to liquefaction at an earthquake magnitude M_W of 7.5. Although the foundation piles have not been considered to obtain any bearing capacity from these soft strata, lateral spreading may result in unforeseen lateral loads on the piles, potentially leading to buckling or bending. Lateral spreading may be possible as the slope of the top of the upper soil stratum approaches 2° from borehole S6 to S3, see Figure 2-5 in Part I.

However, dredging might only be a temporary solution. Due to transport by currents, sediment may build up behind the proposed breakwater, and once again cover the bedrock. Sediment sources include Coliumo Bay itself, primarily, and the Estero Dichato entering the bay on the southern side, as shown in Figure 1-2. Considering that the current levels of sediment atop the sedimentary rock are low this is a long-term problem which requires further analysis of the sediment dynamics of the bay.

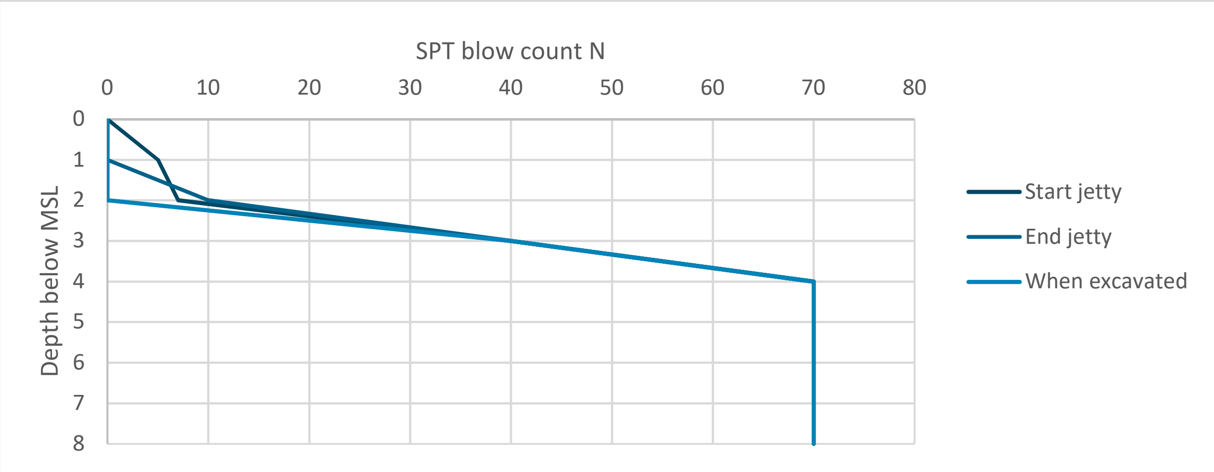

Figure 6-9: SPT blow count with depth for start and end of jetty, and for excavated top soils

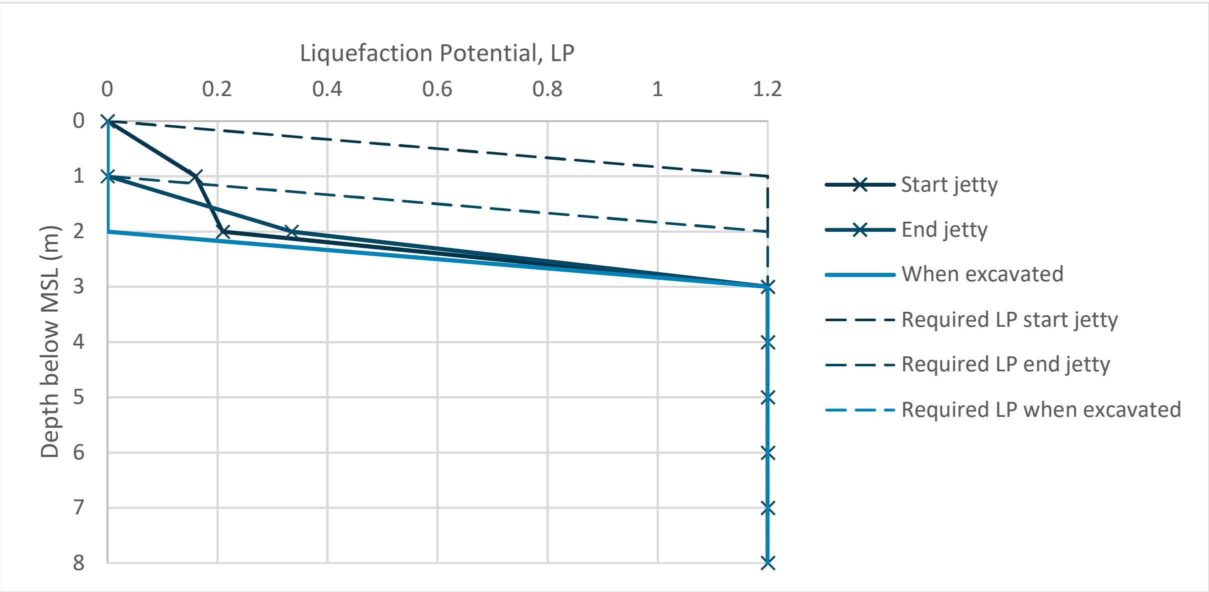

Figure 6-10: Liquefaction Potential in depth and required liquefaction potential values (F.O.S. = 1.2)

Scour

Scour is a special case of sediment transport and occurs when the local transport exceeds the supply from upstream due to a difference in velocity, turbulence, or both (Schiereck & Verhagen, 2012). Insight into the degree of scour is necessary to evaluate the danger of instability of the structure, and whether scour protection is required. *Figure G-21 in Appendix G.6* illustrates the complex three-dimensional flow pattern around a pier. Analytical analysis of scour depths is not possible, so experimental correlations with water depth and pier diameter are used for design. For a first design, the ratio between water depth h_0 and pile diameter D gives an indication of the scour depth h_s, see *Figure G-22 in Appendix G.6*. In the case of the EMBD jetty, with a water depth of 2m and a pile diameter of roughly 0.3m, $\tanh\left(\frac{h_0}{D}\right)$ approaches 1.0, so $h_s \propto D$. Therefore, the scour may develop up to 0.3m in depth.

However, considering the excavatability of the thin silty sand layer overlying the sandstone, scouring is not proposed to present a large problem, especially in the short term. In the long term, due to lack of maintenance, sediment transport, and weathering of the sandstone, a new layer of fine soil may be deposited on top of the rock, but since the piles of the structure do not rely on these layers for bearing strength, scour is unlikely to affect structural stability. Thus, mitigation measures, such as quarry stone, gabion or matted aprons, are not necessary.

6.2.6.3 Structural unity checks on pile

After the preceding considerations for construction and failure mechanisms, the pile design based on Table 6-5 may be optimized. This is done by analysing the adjusted model with ETABS (ETABS, 2016).

According to the software, the governing inclined pile is located at grid point G2 directed in positive y-direction. The corresponding load combination is CS3/5 which resulted into certain forces, as described in Table 6-9. With these data, unity checks can be performed as described in Appendix G.7. The governing unity check has a magnitude of 0.78 for a combination of bending, torsion, shear, and compression. This means that the unity check is fine, and the steel section does not need to be adjusted.

Table 6-9: Governing forces -inclined piles

Load Combination	Axial P	Shear V_x	Shear V_y	Torsion T	Moment M_x	Moment M_y	
CS3/5	-52,577	253	1,081	7,569	247,810	35,929	kgf, cm

The governing straight pile is situated at grid point G3. The associated load combination is CS2/4 which resulted into forces as described in Table 6-10. Unity checks are performed as described in Appendix G.7 The highest unity check equals 1.46 for a combination of bending, torsion, shear, and compression. Therefore, the unity check is not satisfactory and the steel section needs improvement.

Table 6-10: Governing forces -straight piles

Load Combination	Axial P	Shear V_x	Shear V_y	Torsion T	Moment M_x	Moment M_y	
CS2/4	-5,510	7,307	112	7,210	8,264	485,612	kgf, cm

6.2.6.4 Final pile dimensions

Finally, it can be concluded that the inclined piles retain their 362 mm diameter and 6 mm wall thickness. The straight piles needed adjustment and after performing some iterations, it is proved that the dimensions for the straight piles have to be similar to those of the inclined piles. Again, unity checks are executed, as described in Appendix G.7, to prove the adjusted model is satisfactory.

In order to guarantee adequate corrosion protection, the wall thickness of all piles is increased with a value of 4 mm. The resulting profile properties for the piles are shown in Table 6-11. Overall this means that all 25 piles may be ordered of the same diameter, which is economically favourable. The differing length between the two types of steel piles is not a problem, as length may be altered by cutting or welding.

Table 6-11: Profile properties - Ø362/10 *(Instituto Chileno del Acero, 2000)*

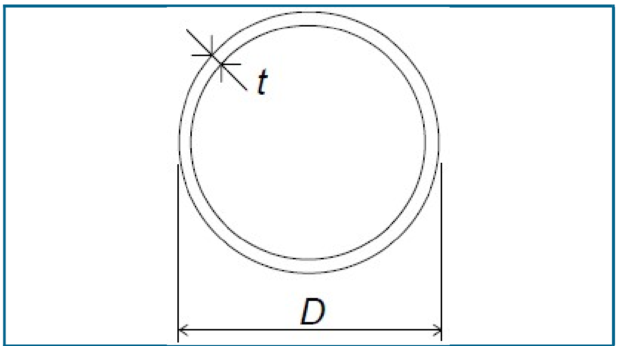

Property	Magnitude	Unity
Diameter, D	362	mm
Wall thickness, t	10	mm
Weight	86.82	kgf/m
Cross-sectional area, A	11058	mm^2
Moment of inertia, I	171410824	mm^4
Number of straight piles	17	-
Number of inclined piles	8 (4x2)	-
Batter angle inclined piles	20	°

6.2.7 Final design: Beams

6.2.7.1 Structural unity checks on beams

From analysing the model using software ETABS (ETABS, 2016) it follows that the beam situated at gridline 2 is governing the design. The corresponding load combination is CS2/1 which resulted into forces, as described in Table 6-12. With these data, unity checks can be performed as described in Appendix G.7. The governing unity check has a magnitude of 0.11 for bending. This ratio is very low, signifying the beam is over dimensioned.

Table 6-12: Governing forces -beams

Load Combination	Axial P	Shear V_x	Shear V_y	Torsion T	Moment M_x	Moment M_y	
CS2/1	0	0	1496	21	285,683	0	kgf, cm

6.2.7.2 Final beam dimensions

After performing some iterations for the beam design, it is concluded to adjust the beam profile to a lower profile, named H300x150x45.8. Again, unity checks are performed, as described in Appendix G.7 to prove the adjusted design is satisfactory. More information about the beam profile can be found in Table 6-13.

Table 6-13: Profile properties -H300x150x45.8 (Instituto Chileno del Acero, 2000)

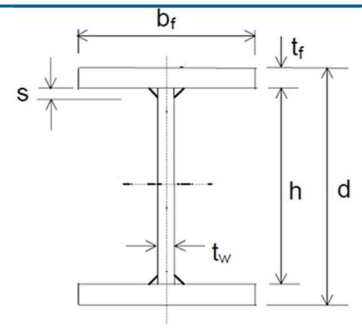

Property	Magnitude	Unity
Height profile, d	300	mm
Width profile, b_f	150	mm
Weight	45.8	kgf/m
Flange thickness, t_f	14	mm
Web thickness, t_w	6	mm
Web height, h	272	mm
Cross-sectional area, A	5832	mm^2
Moment of inertia, strong axis	96000000	mm^4
Moment of inertia, weak axis	7880000	mm^4

6.2.8 FINAL DESIGN: DECK

The concrete deck has been dimensioned at a thickness of 250 mm. For a 5 m × 3 m grid, this is quite a sturdy size. The only thing left to be determined is the amount of reinforcement needed for our structure. For this calculation the code ACI-318-08 (ACI Committee 318, 2008) is followed, using the input provided by software SAFE (SAFE, 2016) as presented in Appendix G.7.

The maximum absolute moment that occurs in the structure is (-) 409251,74 kgf-cm, see Appendix G.7. Following the approach described in ACI-318-08 (ACI Committee 318, 2008), assuming a concrete cover of 60 cm thickness, this requires 9 steel bars of 10 mm thickness per 1000 mm. The final properties are summarized in Table 6-14. For practical reasons, the reinforcement will be designed in the same way in both directions, both at the bottom and at the top of the deck. The final design is presented in Figure 6-11.

Table 6-14: Properties concrete deck and reinforcement

Property	Magnitude	Unity
Thickness concrete	250	mm
Width concrete	1000	mm
Concrete cover	6	mm
Diameter of bar	10	mm
Number of bars	9	[-]

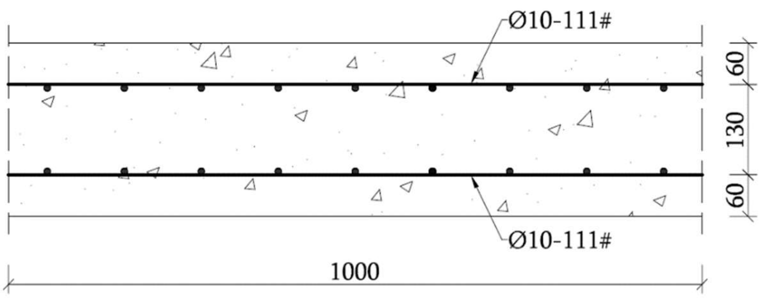

Figure 6-11: Design concrete deck and reinforcement (units in mm)

6.1.8 FINAL DESIGN: DRAWINGS

To summarize all the previous conclusions, some final drawings are attached in the Appendix. First, a floor plan of the deck can be found in Appendix L. This drawing shows the dimensions and the configuration of the steel frame, the steel piles, the concrete deck, the frame of the stairs, and the defenders. The second drawing in Appendix L shows the elevational view of grid line 3 in which the configuration of the stairs and the protection frame becomes clear.

Next, a principle detail is displayed in Figure 6-12. The detail explains the connection between the jetty and the concrete abutment. The jetty and the abutment have different fundamental periods, so it is important they are not attached to each other and can move independently. To guarantee this independency, a gap of 20 mm is created between the two structures. This value is based on about two times the deflection during the event of an earthquake. A steel plate is used to make sure the jetty is still accessible for traffic, but it is only fixed to one end so it can move freely.

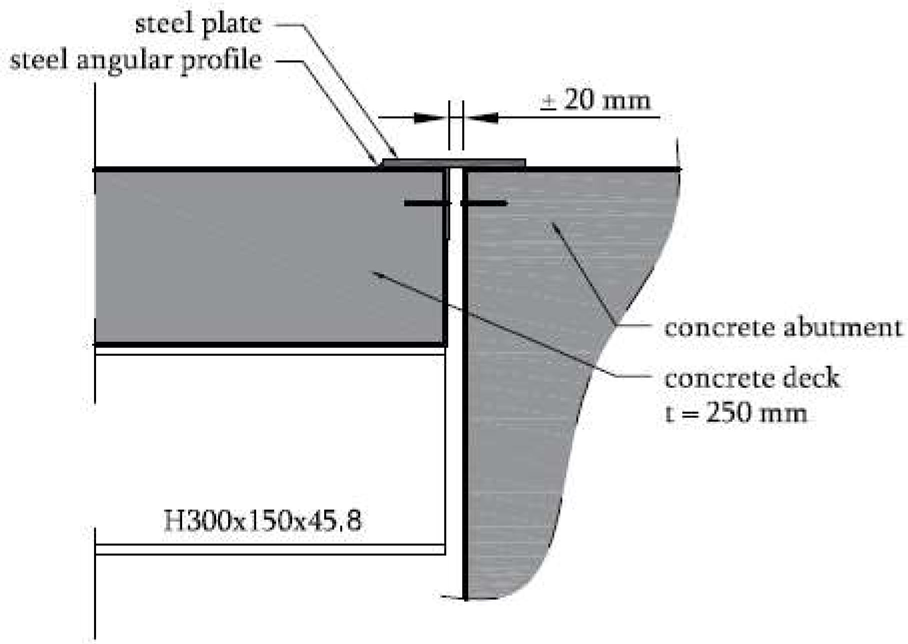

Figure 6-12: Principle detail of the connection jetty-abutment

7 PRELIMINARY DESIGN: BREAKWATER

In this paragraph the design of the breakwater is elaborated. The function of the breakwater within the whole system of the mooring facility is to protect the mooring facility from the incoming waves. This is necessary to create a safe climate to ensure that the facility can fulfil the required mooring functions.

7.1 DESIGN PROCESS

The demensions of the breakwater are first designed against wind waves in the area. After that, a damage evaluation regarding the earthquake and tsunami loads is elaborated in Chapter 9. The 2010 earthquake and tsunami event is taken as the norm. The loads caused by the tsunami and earthquake cannot be withstand against reasonable costs and therefor only damage control should be applied.

A flowchart of the design of the breakwater is included in Figure 7-1. In summary, offshore waves are statistically analysed, using a peak over threshold method and Weibull/ Gumbel transgression. Via this analysis, a return period for the ULS and SLS is determined and a corresponding wave condition. Offshore wave statistics are translated to onshore (taking into account shoaling, dissipation etc.). For a first iteration SwanOne is used, in the second iteration Delft3D is used. The onshore wave statistics in combination with the requirements for SLS and ULS determine the breakwater dimensions. A geotechnical analysis is performed to check the stability and settlements of the breakwater and eventual lead to changes in the design of the breakwater.

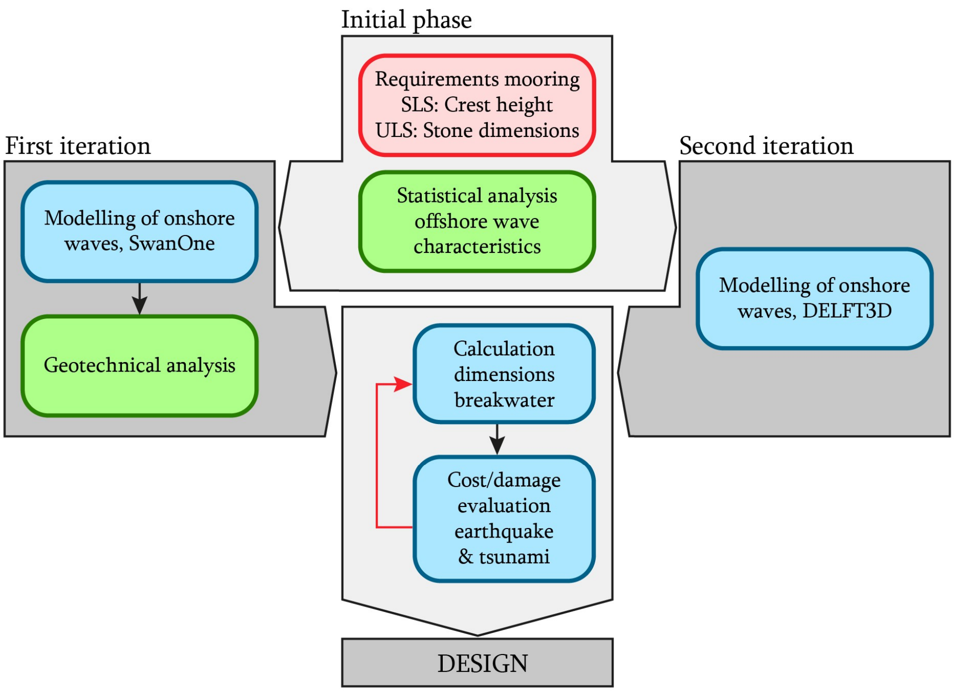

Figure 7-1: Flow diagram for breakwater design process

7.2 REQUIREMENTS

In the design of the breakwater, basically two different cases have to be distinguished. The breakwater needs to protect the jetty from incoming waves, more specifically it needs to keep the waves low for the mooring of the ship. This results in an allowable overtopping or wave transmission of the breakwater (made clear in Figure 7-2). The allowable wave transmission is dependent on the serviceability limit state (SLS). In other words, the allowable downtime for the jetty determines at how many days this transmitted wave height may be exceeded. The stone size however depends on the ULS. This means, the stones may not become unstable before the ultimate limit state is reached. This is a rather traditional Dutch approach. The Chilean experience will be implemented in the damage evaluation (of the tsunami and earthquake) afterwards, where damage is accepted.

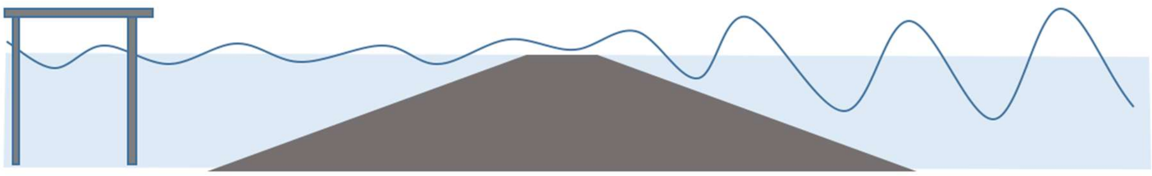

Figure 7-2: Breakwater principle

7.2.1 OFFSHORE WAVE CHARACTERISTICS

The offshore waves, before being translated onshore, are as described in the boundary conditions, mainly waves from two distinct directions. A comprehensive analysis on the wave directions is worked out in Appendix H.1. In this analysis different scenarios are elaborated. Offshore wave heights are calculated using Weibull, Gumbel and a peak-over threshold analysis. Scenarios with narrow angle and a broader angle are used, because of the different outcomes. The highest values will be used for the design, to be conservative. The outcome off this analysis is summarized in Table 7-1.

Table 7-1: Offshore wave heights, outcome for a narrow (NW and SW) and broad (NW-N and S-W) angle

		Average Gumbel-Weibull			
		SLS	Tp SLS	ULS	Tp ULS
Small	NW	2,96	7,5	9,16	12
Large	NW-N	4,11	9	10,25	13,3
Small	SW	5,39	13,5	10,58	17,5
Large	S-W	5,80	13,5	10,26	17,5

7.2.2 ONSHORE WAVE CHARACTERISTICS

In this second iteration, the offshore wave height is translated to an onshore wave height using Delft3D. With Delft3D the detailed bathymetry of Dichato bay can be taken better into account than with SwanOne in the first Dimensioning step. A comprehensive explanation of the wave translation by DELFT3D is given in Appendix H.2.

The scenario study makes clear that the waves from the North-Western create the governing wave conditions in Coliumo bay both for the ULS and SLS. The results of the governing scenarios are presented in Figure 7-3, Figure 7-4 and Table 7-2.

Table 7-2: with translated wave heights (ULS and SLS) onshore.

	Scenario	Hs Offshore [m]	Hs Onshore [m]	Depth [m]	Tm01 [sec]
ULS	NW-N_ULS	10,25	4,49	4,76	10,74
SLS	NW-N_SLS	4,11	1,71	5,36	6,45

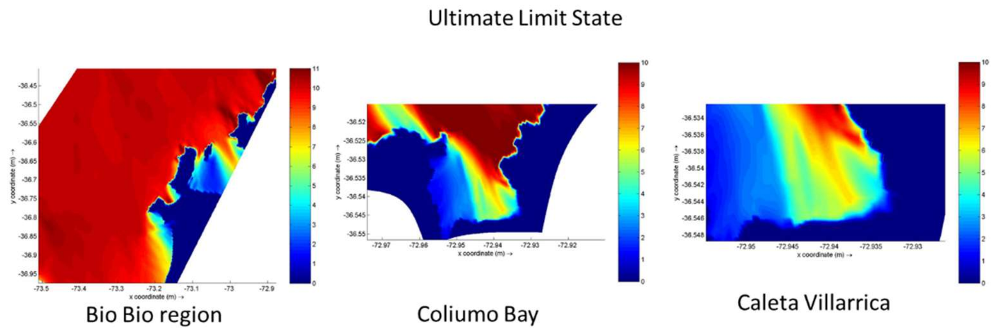

Figure 7-3: Ultimate Limit State, Outcome Delft3D, , more detail from left to right

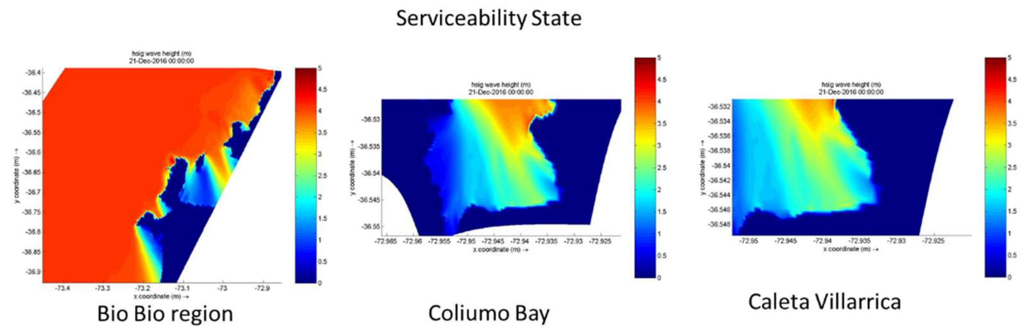

Figure 7-4: Serviceability Limit State with north-western waves, Outcome Delft3D, more detail from left to right

7.2.3 CREST HEIGHT

The downtime of the jetty is set on 5% per year, which is decided in the program of requirements. This downtime results in an acceptable non-service of 18 days a year (Serviceability Limit State). This non-service means that the ship can stay moored if it is moored, but the mooring process itself is impossible according to the guidelines. The guidelines give a limit of 0,30m wave height in the harbour area for ships of this size (Wijdeven, 2015). Hence, the annual probability is 18 days a year, so on average 18 days a year there is a significant onshore wave height of 1.71 m.

With help of the software BREAKWAT3.0 (Software of the Deltares), a calculation of the crest height is made, based on the before mentioned wave transmission. Some assumptions are made regarding different parameters. A more detailed outcome is given in Appendix H.3.

The height of the breakwater is calculated on **+2.56m MSL**, using BREAKWAT3.0.

7.2.4 STONE DIMENSIONS

The (ULS) storm wave height is a value based on a probability of failure and the lifetime of the structure. In this case the lifetime is set on 25 years and the probability of failure under normal storm conditions (no tsunami conditions) is 10%. This is a rather average value in the range of 5%-20% (Verhagen, d'Angremond, & van Roode, 2009). These values refer to a design storm of about once every 250 years, sea Appendix H.1.

In this second iteration, the wave height offshore is translated to an onshore value using Delft3D. The results are listed in Table 7-2. Using the software BREAKWAT3.0, the stone size is determined. The outcome and calculations of BREAKWAT3.0 can be find in Appendix H.3. A weight (W50) of **10.000 kg** is obtained, with an average diameter of **1.56 m.**

7.2.5 BREAKWATER DESIGN

The breakwater design is rather simplistic. The breakwater is founded on a rock layer, which is not very usual in breakwater design. Therefor no filter layers are necessary, as well as no toe- and scour protection (because there is no outwash of material). Assumed is a slope of 1:2 and a crest width of about 3 stones (4,5m). Because the Chile is a tsunami prone area the breakwater is just made out of one stone dimension, this will be discussed in Chapter 9. The basic design of the breakwater in summarized in Table 7-3, Figure 7-5 and Figure 7-6.

Table 7-3: Design breakwater

Crest freeboard (above HWL)	1.45 m
High tide	+1.11m MSL
Height breakwater	+2.56 m MSL
Length	40 m
Crest width	4.5 m
Average height crest (from seabed)	+6.06 m MSL
Slope	1:2
Average cross section	82 m^2
Total volume	4600 m^3
W50	10.000 kg
Dn50	1.56m

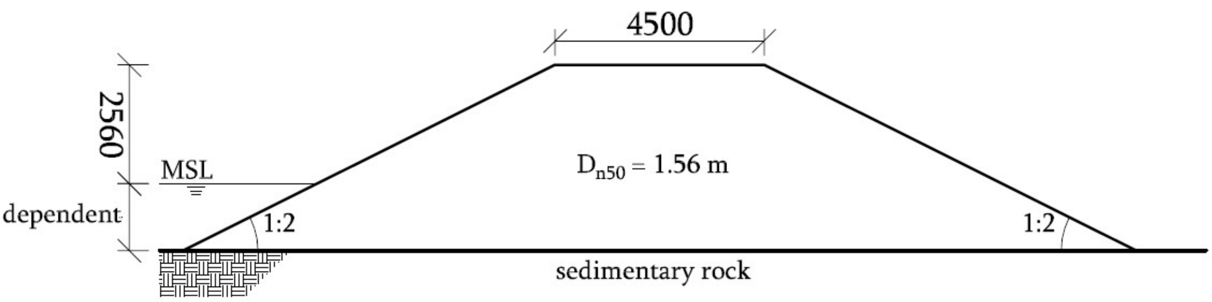

Figure 7-5: Dimensions of breakwater in [mm]

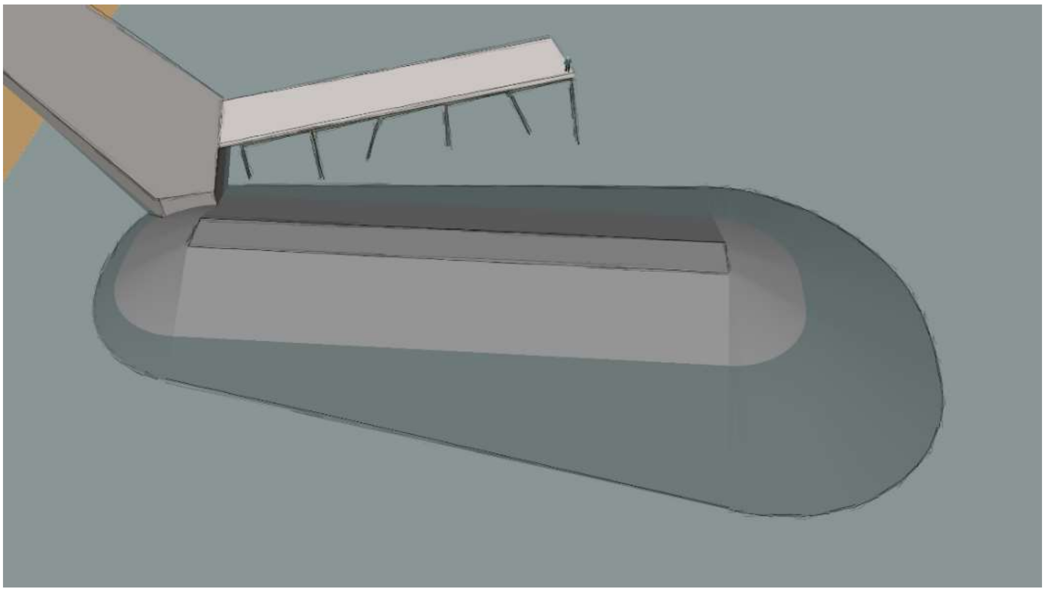

Figure 7-6: 3D visualisation of breakwater design. The waves are perpendicular on the breakwater, with their origin at the bottom of the figure.

7.2.6 DIFFERENCES WITH FIRST ITERATION

The main difference in the second iteration (Appendix H), compared to the first iteration (Appendix F), are the stone dimensions. The stone dimensions have increased by a factor 2 (weight factor 10), whereas the crest height was estimated quite well (except for the fact that the tide analysis is improved, which leads to a higher high tide). The stone dimensions are so much bigger because of the DELFT3D model, who is more accurate in calculating waves in detailed bathymetry, such as the Coliumo bay. DELFT3D calculated an onshore wave height of 4.5m, instead of the 2.0m of SwanOne. Another explanation for this increased wave height is a changed input due to a comprehensive wave direction analysis.

7.2.7 DEFORMATION AND PORE PRESSURES: PLAXIS2D

PLAXIS 2D is used to evaluate the stability and settlement behaviour of the breakwater under its own weight, and a flow-only computation is made to analyse the impact of the significant wave on pore pressure development in the breakwater. To analyse the influence of the subsoil conditions on the settlement of the breakwater two situations are investigated: 1) where a soft sandy layer overlies the sandstone 2) where the sandy layer has been dredged and the breakwater rests directly on the sandstone.

Overall, the breakwater settlement is minimal under gravity loading, and ranges between 10 and 30 mm depending on whether the sand layer is removed or not. The sand layer allows for more deformation and the global stability of this configuration is a factor 1.3 less safe than if the layer were to be removed. However, both configurations have acceptable factors of safety against global failure. In terms of pore pressure build-up during harmonic wave loading, the generated pore pressures at the toe of the breakwater are generally 4 times higher than those at the breakwater. Also, the presence of the sandy layer in soil scenario 1 dampens the pore pressure build up, as it is more porous than the sandstone.

The dimensions used for the breakwater as modelled in PLAXIS2D stem from the dimensioning phase (i.e. first iteration) of the breakwater design. However, it is not deemed necessary to conduct a secondary analysis considering the limited required incresae in crest height (2.2m to 2.56m) and the relatively limited settlement, especially when the soft soils are removed. See Appendix H.4 for the full results and visual output from PLAXIS 2D.

8 PRELIMINARY DESIGN: ONSHORE FACILITIES

8.1 EBMD BUILDING

8.1.1 CHILEAN PRINCIPLES

In his lecture of December 16, 2016, architect Mr. Baeriswyl explained the basic architectural principles of his master plan for the Dichato area Damage is acceptable (Baeriswyl, 2015). However, after the occurrence of an earthquake and tsunami, the main goal is to provide an efficient rehabilitation. This can be ensured by lifting the first line of structures on the coast up by applying poles on the ground floor and by applying a robust core comprising all main functions the building needs.

8.1.2 APPROACH

For the well-functioning of the Marine Biology Station, the redevelopment of the biggest structure on-site proves to be the most relevant to look at, see Figure 8-1. As the remnants of the building are heavily deteriorated, the structure will be stripped to its basic structural elements. The stability will be improved, but it will be kept structurally "open" in case a tsunami occurs. An additional partial layer will be built on top, which will be completely structurally independent. A strong core will be constructed, comprising a staircase and service elements such as water pipes and electricity facilities. The underlying principle is that the core will not be damaged in case of an earthquake and tsunami, thus enabling quick redevelopment of the building's functions. The step-by-step redevelopment is presented in Figure 8-4 to Figure 8-10.

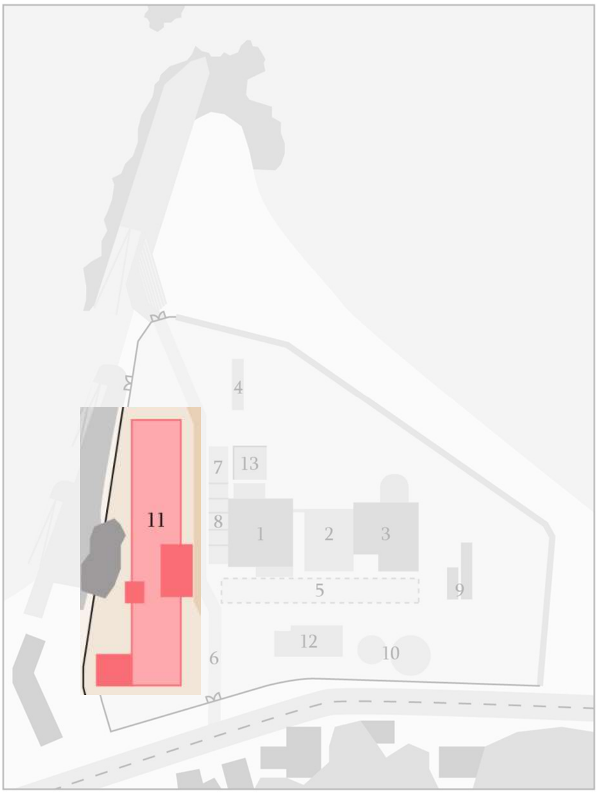

Figure 8-1: Location of redevelopment building

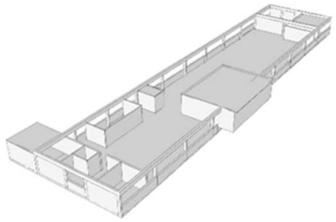

Figure 8-2: Current situation

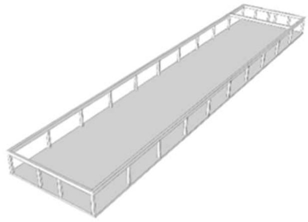

Figure 8-3: Strip to basic structure

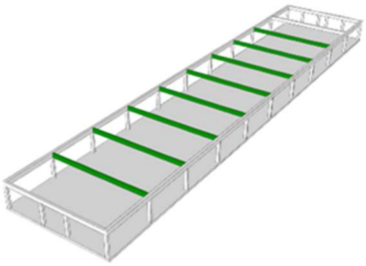

Figure 8-4: Rebuild structural frame

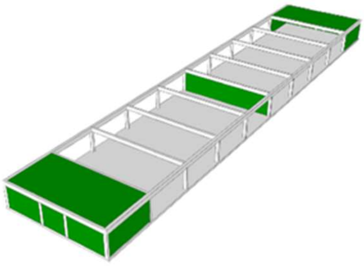

Figure 8-5: Apply stability elements

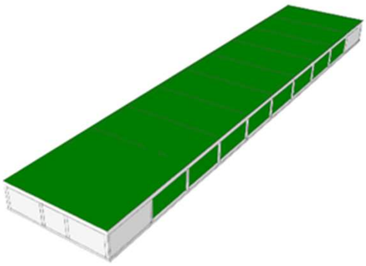

Figure 8-6: Apply light-weight dividers

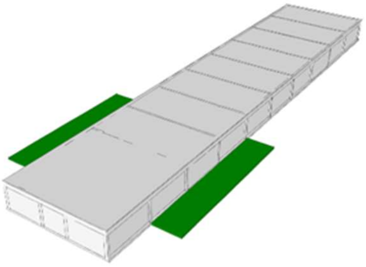

Figure 8-7: Construct additional shallow foundation

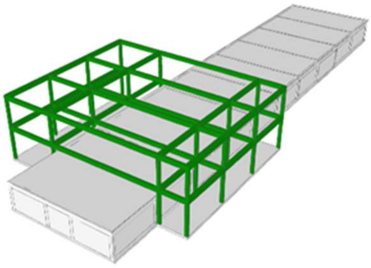

Figure 8-8: Construct independent frame

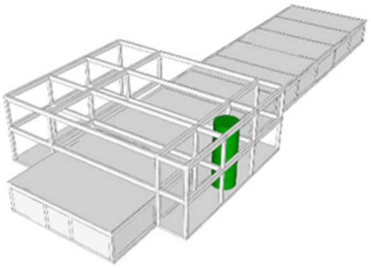

Figure 8-9: Apply robust core

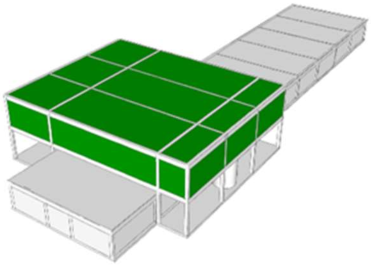

Figure 8-10: Construct stable walls, floor and roof

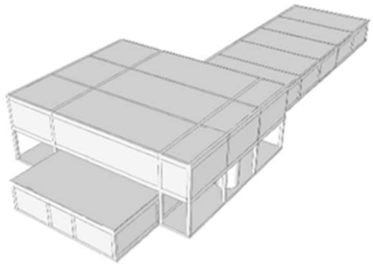

Figure 8-11: Final principle design

8.2 Pavement

8.2.1 Current pavement and design criteria

Currently at the Marine Biology Station, an unpaved sandy road runs down from the coastal road *Costanera Pedro Aguirre Cerda*, marked in dark grey and light grey Figure 8-12, respectively. The traffic on the unpaved road is and will remain light: a single ¾ truck. The loads imposed by the truck on the pavement is 50 kN in total, including its maximum loading capacity. The force is transferred via the wheels, which are spaced 2.03m apart axially and 3.60m apart longitudinally. Since the unpaved road has been used by the truck since 1978, the subgrade soil is well-compacted.

The current problems with the unpaved road include:

- The serviceability level of the gravel road may vary significantly within short periods of time, for example, due to heavy rainfall.
- A high level of maintenance is required to maintain the appropriate levels of gravels. However, this maintenance is not carried out.
- Truck transit on the road produces substantial dust emission, which is an impairment to staff and students at the Marine Biology Station; to the natural surroundings (plants, crops, outside aquaria etc.); and to facilities and machinery on site.
- Drainage is insufficient during the winter season.

The design criteria for the Marine Biology Station pavement are:

- To allow one ¾ truck to transit goods from the Costanera Pedro Aguirre Cerda road to the jetty, and vice versa;
- To incorporate the possibility of reinforcing the pavement for an increase in traffic volume (i.e. multiple trucks) without significantly altering the existing pavement structure;
- To ensure mobility of the vehicle(s) during all seasons of the year;
- To ensure pedestrian safety and;
- To control the emission of dust.

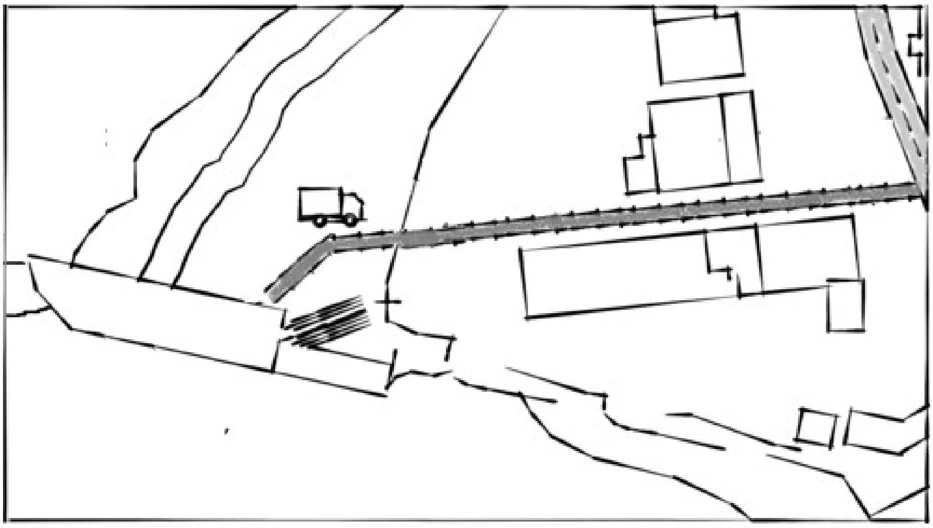

Figure 8-12: Overview infrastructure Marine Biology Station

8.2.2 Design methodology

A design is made for a low-volume traffic road according to the Chilean guideline *Guía de Diseño Estrucutral de Pavimentos para Caminos de Bajo Volumen de Tránsito* (2002). The full methodology is given in Appendix I. Design: Pavement.

8.2.3 Pavement design

Following the Design Option 2 of the pavement structure highlighted in Figure I-2 in Appendix I, the road consists of 12 cm of granular subbase of CBR 50%, topped by 16 cm of granular base of CBR 100%, in turn covered with a surface treatment layer.

Table 8-1: Material for pavement layers

Pavement layer	Thickness (cm)	Material	Source
Granular subbase CBR 50%	12.0	Reclaimed Concrete Material, RCM[3]	Demolished concrete skeleton of old Marine Biology Station building
Granular base CBR 100%	16.0	Crushed granitic rock	Waste material from armourstone quarrying
Surface treatment	1.0	Microsurfacing[4]	Emulsified asphalt, fine aggregate and mineral filler (Portland cement)

8.2.4 Compaction and drainage

It is assumed that the subgrade is well-compacted due to previous use. Compacting the subgrade further is of little use, as compacting mainly influences the cohesion of a soil, and the angle of internal friction only minimally. For coarse-grained granular subgrade without cohesion extra compaction will not significantly improve performance.

Moisture content, on the other hand, influences both the cohesion and the angle of internal friction of the subgrade. A Proctor test may determine the optimal moisture content for each pavement layer for maximum compaction. Water ingresses into the pavement and subgrade due to capillary movements or rainfall infiltration and may weaken the material. In terms of drainage, the groundwater table is near-surface, and therefore subsoil drains may be ineffective, as it is difficult to provide an outlet. For surface drainage it is most cost-effective to induce a transversal or longitudinal slope in the pavement of 2-4% to allow for run-off.

[3] Requires processing and washing to remove fines which could plug drains or cause leachate precipitation.
[4] Blend of emulsified asphalt, water, well-graded fine aggregate and mineral filler. Requires maintenance every 5-7 years.

9 EXTREME IMPACT EVALUATION

9.1 APPROACH

What differentiates the design of coastal structures in Chile from design elsewhere, is the need to take into account extreme events, such as earthquakes and associated tsunamis. A common scenario for coastal structures during an extreme event (large-scale seismic event) is to experience one or more seismic shocks, followed by subjection to multiple tsunami waves within the next few hours, i.e. the tsunami impacts an already deformed or otherwise damaged structure.

In general, structural design in Chile is carried out according to codes which ensure life safety during earthquake events, by considering ranges of seismic loading. For tsunamis, on the other hand, design generally assumes evacuation of all people, and focuses on structural damage minimization.

In an Extreme Impact Evaluation, it is important to consider the idea of *risk*, since it may not be possible to design structures to fully withstand all extreme impacts at all times. Risk may be defined as the combination of the likelihood of occurrence of an extreme event and the associated level of damage it may induce. For the following evaluation, the extreme event of the Maule 2010 earthquake and tsunami is taken as a base case, given the amount of available data of this event and the previously investigated impacts on the Dichato coastal area.

The following evaluation thus investigates the impact of the Maule 2010 earthquake on individual elements of the EMBD design proposal -including the jetty, the breakwater and onshore facilities- followed by an investigation of the effects of the subsequent tsunami waves. The jetty and breakwater are evaluated on structural stability. Furthermore, several geohazards are treated for the jetty, the breakwater and onshore facilities.

9.1.1 GEOHAZARD ANALYSIS

Geohazards may be defined as geological and environmental conditions or states that may lead to widespread damage or risk (IIASA, 2015). The Extreme Impact of scope in this chapter concerns the seismic event of 2010 –the Maule earthquake and tsunami. See Appendix A.2-A.8 for information on earthquakes, tsunamis and the relation between these events and Chile. The geohazards resulting from seismic events, specified to the Marine Biology Station, are treated in the following chapter, and mitigation measures are suggested for each.

From the Maule 2010 earthquake experience the following geotechnical effects emerge which may affect the harbour complex (Yasuda, Verdugo, & Konagai, 2010):

- Cracking or failure of the connection between the foundation and the superstructure;
- Differential uplift and subsidence;
- Liquefaction and lateral spreading-induced damage including settlement and foundation failure;
- Slope and embankment failures;

- Damage to harbour structures, induced primarily by differential deformation between the offshore foundation and land side connection. Soil-structure interaction is a critical phenomenon here;
- And tsunami induced effects which differ according to local topography, and may include scouring.

Figure 9-1 depicts, conceptually, various geohazards which may affect the Marine Biology Station. Due to the relatively thin sand layer overlying the sedimentary rock at Dichato, the amount of seismic amplification through the soil is limited. This means the structural damage of onshore buildings from deformations caused directly by seismic acceleration is unlikely to be problematic. Indeed, the Maule 2010 event proved that the majority of the damage was caused by either liquefaction-related phenomena and the tsunami ensuing the earthquake.

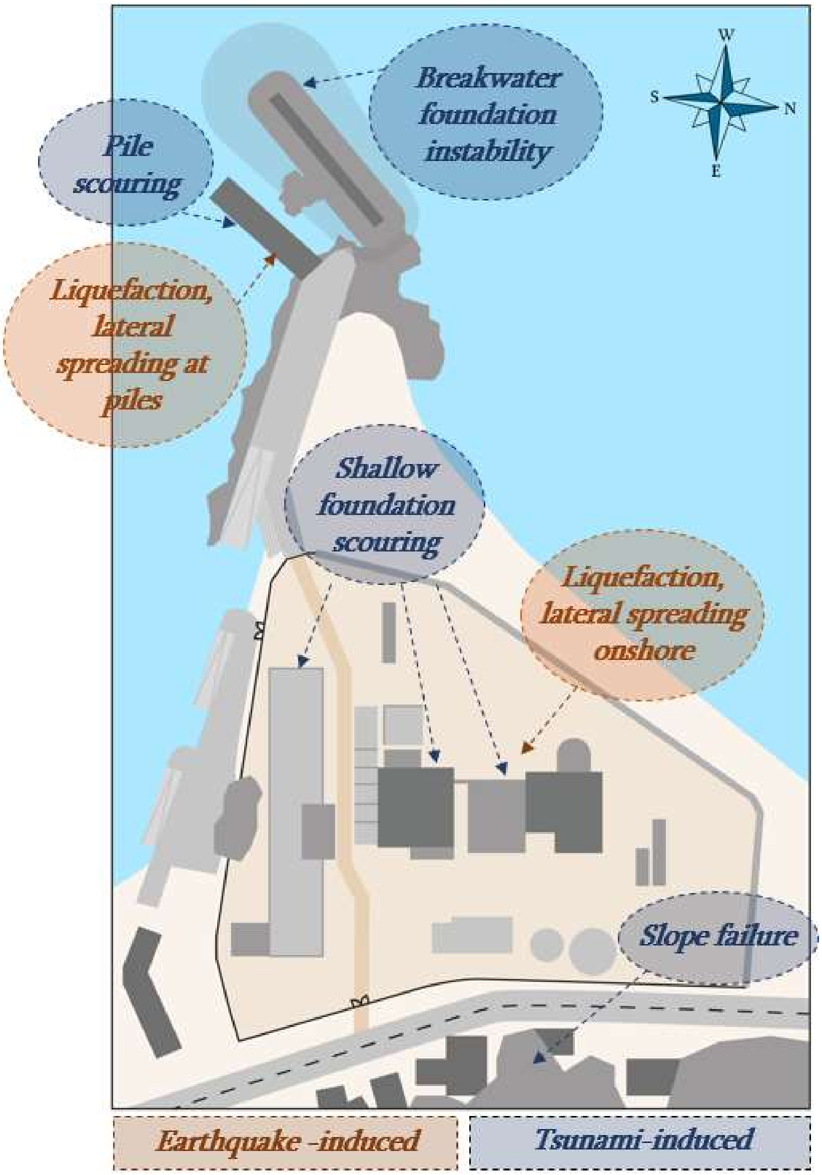

Figure 9-1: Overview of potential geohazards at Marine Biology Station

9.2 EARTHQUAKE DAMAGE

Structures are affected mainly by surface waves resulting from a seismic event, which exert extreme horizontal forces on standing structures. Sudden lateral accelerations generate significant stresses in structural elements as well as their connectors. The level of damage to a structure depends on the subsurface, foundation type, structural ductility and strength, amongst others. See Appendix A.5 for more information of seismic design philosophies.

Often it is not feasible to design a structure to such an extent in which it does not show any damage after the event of a heavy earthquake. The design is therefore limited in achieving two important objectives (Hidalgo, Norma Chilena Oficial Nch2369.Of2003, 2003). First, protection of people's lives needs to be guaranteed. In achieving this, structures may not collapse, fires should be avoided, and the emission of toxic gases and liquids need to be limited. Secondly, the operation of the jetty and breakwater cannot be obstructed for a long period of time. Essential processes may not be interrupted or come to a standstill and the structure should still be available for inspection and repair.

What has become clear until now, the occurrence of heavy earthquakes is not negligible in Chile. In this report, special attention has been paid to the Maule earthquake of February 2010. Details have already been discussed in Appendix A.8. All geohazards are evaluated using this M_w 8.8 earthquake. However, the damage to the jetty and breakwater are evaluated using seismic loads according to the code, and not using the acceleration spectrum of Maule 2010, because the Chilean codes already incorporate large-scale earthquakes such as Maule 2010 in the computation of seismic loads.

9.2.1 JETTY

9.2.1.1 Structural damage

First and foremost, the influence of the earthquake on the jetty will be discussed. Before the extreme event of February 2010, the codes for seismic design in Chile were already of good quality. For this reason, structural damage was relatively small even with the high ground accelerations of 0.65g that have been measured. After the event, again new experiences have been gained and the codes got even better improvement. The current Chilean seismic codes, which are also used in the design of this project, take into account extreme and heavy earthquakes. Because of the lack of possibilities and time to perform a dynamic analysis including the Maule earthquake, it is decided to adhere to the seismic static loads calculated according to the Chilean seismic codes.

In the design of the jetty, seismic load combinations which contain seismic loads from the codes have been used. In the final design, all unity checks are fine which means that the structure will both survive an earthquake and only elastic deformations will occur. For this reason, it can be concluded there will be no permanent deformations in the structure when the tsunami arrives.

9.2.1.2 Geohazard: Liquefaction and lateral spreading

See Chapter 6.2.7.2: Failure Mechanisms and the corresponding Appendix G.4 for computations of liquefaction susceptibility at the jetty piles, for an earthquake with magnitude 7.5. It was concluded that liquefaction or lateral spreading are not hazardous when the top soil is excavated to MSL -2m at the proposed jetty location. However, for the Extreme Impact Evaluation, the moment magnitude under consideration is 8.8. The revised Idriss scaling factor for factor of safety against liquefaction to correct for magnitude is

$$FS = (CRR_{7,5}/CSR)MSF$$

With

$$MSF = 10^{2.24}/M_w^{2.56}$$

Giving an MSF for a 8.8 M_w earthquake (like Maule 2010) of 0.664. This means the Liquefaction Potential values as in *Figure 6.9 in Chapter 6.2.7.2* becomes almost twice as unfavourable for the sand lying atop the sedimentary rock. For the underlying rock, i.e. from a depth of 3m below MSL downwards, the liquefaction potential remains satisfactory. Therefore, as long as the top 2m of soil is removed at the jetty location, there is no liquefaction hazard for pile stability in the case of a seismic event like that of Maule 2010.

9.2.2 BREAKWATER

9.2.2.1 Earthquake loads

During the extreme impact event, a maximum acceleration of 0.4g m/s² is observed (see Appendix G.4.2). The consequences of this 'force' on the breakwater is widely investigated around the world. The design of the breakwater is adapted to several conclusions of these reports;

- (Wang, Yang, Lamison, & Chen, 1978)
  - Breakwaters on a rigid foundation are highly earthquake resistant
  - An earthquake of less than 0.5g m/s² would not affect the breakwater to any significant extent.
  - The failure mode is binary; settlement of the crest and a slope deformation.
- (Yang & Jin, 2015)
  - The earthquake has a high effect on the hydrodynamic pressure in a breakwater is the permeability is low.
- (Memos, Bouckovalas, & Tsiachris, 2012)
  - Rubble-mound breakwaters are quite seismic resistant is resting on a rigid bed. Only when founded on a soft bed, extra care during design should be taken.

The breakwater at the Marine Biology Station is founded on a very stiff soil, the sandy top soil of 2m is dredged. Also in the design no core is implemented, to make the breakwater permeable. This is important to avoid high pressures in the breakwater during earthquake (and tsunami) impact. The final result of an earthquake is a settlement of the crest, which will be low according to the literature because of the rigid foundation. The MCE (Maximum Considered Event) is estimated to occur every

2500 years (which has just happened in 2010) and therefore, no further adjustments to the breakwater are necessary for the earthquake loads. Also, no extensive calculation is carried out for this reason. This might be necessary in future research and more detailed designing of the harbour facility.

Another reason to pay not too much attention to the exact settlement of the breakwater is the fact that a tsunami is likely to occur after an earthquake. The tsunami will damage the breakwater more, as is explained in Chapter 9.3.2.

9.2.3 Onshore structures

9.2.3.1 Geohazard: Liquefaction and lateral spreading

The educational and research facilities part of the Marine Biology Station are founded on shallow foundations consisting of concrete slabs resting on a sandy soil. Liquefaction induced settlements are not a problem for the foundation per se, but if different settlements occur due to lateral spreading, for example, unallowable rotations and strains could be induced in the concrete slab and its superstructure.

Liquefaction

To evaluate this hazard, the liquefaction potential of the top 3m of soil as identified in the geophysical site test is computed. The input data is derived from the geophysical test performed in December 2016 at Caleta Villarrica and laboratory test performed on sand from Dichato in the soil mechanics laboratory of UdeC in previous years. The sand is classified as medium dense gravelly sand (SW)[5]. The liquefaction potential is calculated as in Appendix G.4 (corrected for magnitude 8.8 as opposed to 7.5) and is summarized in Table 9-1. In order to obtain a satisfactory factor of safety against liquefaction (LP of 1.2), the blow count would need to become at least N=18[6], but generally a minimum N-value of 30 is recommended by the ASTM guidelines of the U.S. In seismically active regions.

Liquefaction may cause unallowable levels of settlement of the ground surface and correspondingly the shallow foundations and the overlying superstructures. Yoshimine et al. (2006) have found a relationship between the volumetric strain and shear wave velocity of a soil, for given factors of safety against liquefaction, see Considering the factor of safety of 0.78 as given in Table 9-1, and a shear wave velocity of the top sand layer of around 190 m/s (see Figure B.10 in Appendix B.4.3), one can deduce a post-liquefaction volumetric strain ε_v of 2.5 %. For the sand layer of 3m depth this accounts for 7.5mm of settlement. For residential buildings on shallow foundations in the Netherlands[7] settlement restrictions lie at 0.10m for the Ultimate Limit State and at 0.03m for Serviceability Limit State (NNI, 2006). Therefore, the SLS would not be satisfied in the case of liquefaction-induced settlement.

[5] According to USCS: Unified Soil Classification System

[6] In this case LP would become 1.34

[7] Restriction values were not specified in the Chilean design code

Lateral spreading

Lateral spreading may follow liquefaction and as the ground tears and surface fissures open up, lateral forces may be induced in the concrete shallow foundation, causing it to extend and potentially crack. There is around 8 m difference in elevation from one end of the Marine Biology Station to another (from the sea-side at the concrete abutment to coastal road), which is a distance of approximately 100m. This results in an inclination of 4-5° on average, which is a theoretically sufficient inclination to undergo lateral spreading (Haigh, 2000).

Mitigation

To mitigate the risk of structural damage in the concrete slab due to lateral spreading it is important to ensure sufficient reinforcement to resist tensional loads by incorporating safety factors in the design. Overall, in order to reduce the impact of liquefaction and associated lateral spreading, the sand may be densified. The required increase of SPT blow count of the sand may be achieved through densification by dynamic compaction, for example. This is a technique often applied to mitigate liquefaction in loose saturated granular soils, and involves high-energy impacts to the ground surface by systematically dropping heavy weights from heights ranging between 10 and 40 m using heavy crawler cranes. An impression is given in Figure 9-3.

Table 9-1: Summary of liquefaction potential calculation for onshore soil

Input parameters		Output	
γ_{sat}, kN/m³	19.5	CSR	0.256
γ_{unsat}, kN/m³	9.5	CRR	0.302
% fines	10	Liquefaction Potential, LP	0.784
SPT blow count, N	15		
Depth of evaluation, m below surface	1		
Magnitude scaling factor	0.664		

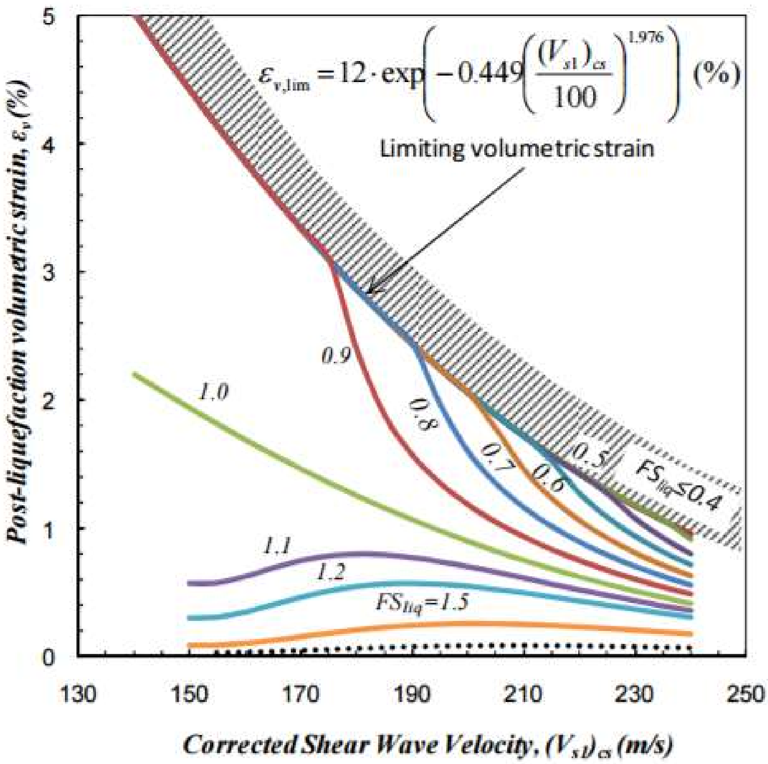

Figure 9-2: Relationship between volumetric strain and shear wave velocity for a given factor of safety against liquefaction with limiting volumetric strain

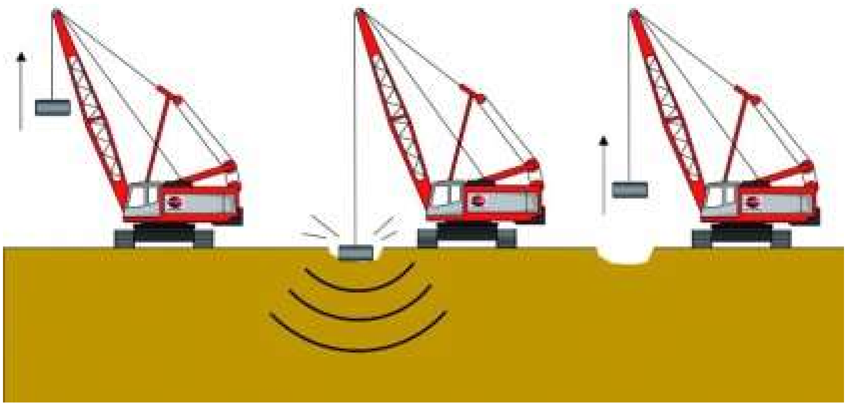

Figure 9-3: Impression of dynamic compaction method used to mitigate liquefaction

9.3 TSUNAMI DAMAGE

In this part the effects of a tsunami are evaluated. There is tried to get insight into the behaviour of the design during a tsunami and to make an estimation of the potential damage. To introduce this part and description of the phenomenon Tsunami is cited from section 7.2.2 of the FEMA P-55 Coastal Construction Manual (FEMA, 2011):

"Tsunamis are long-period water waves generated by undersea shallow- focus earthquakes or by undersea crustal displacements (subduction of tectonic plates), landslides, or volcanic activity. Tsunamis can travel great distances, undetected in deep water, but shoaling rapidly in coastal waters and producing a series of large waves capable of destroying harbor facilities, shore protection structures, and upland buildings... Coastal construction in tsunami hazard zones must consider the effects of tsunami run-up, flooding, erosion, and debris loads. Designers should also be aware that the "run-down" or return of water to the sea can also damage the landward sides of structures that withstood the initial run-up."

The tsunami forces are evaluated using the maximum known event. This event is called MCT (Maximum Considered Tsunami). In case of the Coliumo bay, the MCT is defined by the tsunami caused by the Maule earthquake of February 2010. The damage evaluation is based on the numerical model of the tsunami of 2010 (Martinez & Aranguiz, 2016). According to the outcome of the model study, the Maule earthquake caused a tsunami event with waves up to a height of 7 meters, see Figure 9-4.

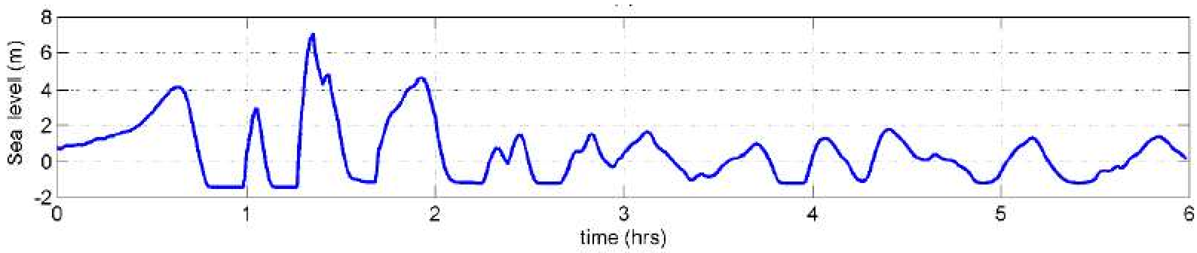

Figure 9-4: Sea level elevation during the tsunami of February 2010 (Martinez & Aranguiz, 2016)

The maximum inudation during the tsunami event is depicted in Figure 9-5.

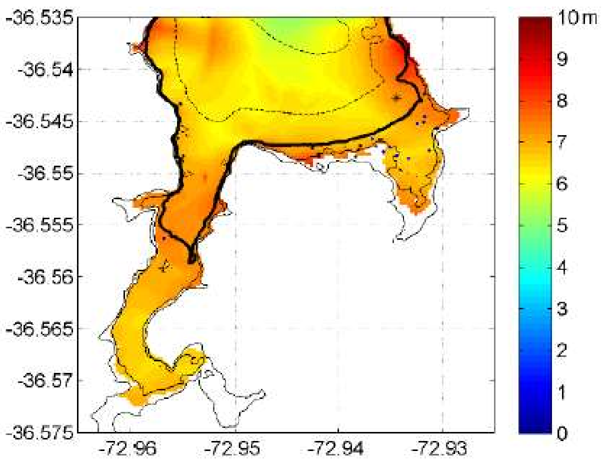

Figure 9-5 Inundation area obtained in the numerical simulation (Martinez & Aranguiz, 2016)

According to the *Risk and design philosophy* described in Chapter 2 of Part I: Analysis, the performance level of the design for this extreme events is: Ensure life safety and minimize the economic damage. To ensure life safety, an evacuation procedure has to be elaborated. The evacuation procedure is beyond the scope of the report. Conversely an evaluation of the economic damage is elaborated.

The damage evaluation starts with the determination of the different loads which are caused by the tsunami. The loads of the tsunami are calculated according to the FEMA (North-American) standards. The FEMA P-646 (FEMA, 2008) describes all the different loads on buildings caused by tsunamis. The loads acting on the breakwater and the jetty during the MCT are summarized underneath. This are the loads of importance for evaluating the potential damage caused by the MCT. An extensive description of the loads is given in Appendix J.1.

- hydrostatic forces;
- buoyant forces;
- hydrodynamic forces;
- impulsive forces;
- debris impact forces;
- debris damming forces;
- uplift forces; and
- additional gravity loads from retained water on elevated floors.

For both the breakwater and the jetty the different forces are determined. Depending on the forces a distinction is made between the different parts of the jetty. The forces on the jetty are shown in Table 9-2. The forces on the breakwater are shown in

Table *9-3*. The effects of the above presented loads are elaborated for both the jetty and the breakwater in upcoming parts.

Table 9-2. Tsunami forces acting on the jetty.

Jetty	*Piles*		*Deck*		*Total structure*	
Force	value	unit	value	unit	value	unit
Hydrostatic	14,47	kN/m length	23,84	kN/m width		
Hydronamic	14,87	kN/m length	22,59	kN/m width		
Impulsive	22,3	kN/m length	33,88	kN/m width		
Debris Impact					1230	kN
Buoyant					3,71	kN/m2
Debris damming					492,76	kN
Uplift					0,3	kN/m2
Additional gravity					61,8	kN/m2

Table 9-3: Tsunami forces acting on the breakwater

Breakwater		
Force	value	unit
Hydrostatic	15,1	kN/m width
Buoyant	42,4	kN/m width
Hydronamic	41,1	kN/m width
Impulsive	61,6	kN/m width
Debris Impact	1230	kN

9.3.1 JETTY

9.3.1.1 Structural damage

As already explained in the previous section, the effect of the tsunami on the jetty will be analysed. Different tsunami load cases are defined and calculated. Not all tsunami loads will take place at the same time, consequently tsunami load combinations are composed. According to FEMA, P-55 Coastal Construction Manual (FEMA, 2011) the tsunami load combinations can be defined as displayed in Table 9-4. See Appendix J.6 for more detail. The configuration of the tsunami loads is visualized in Figure 9-6.

Table 9-4: General tsunami load combinations

	D	L	F_h	F_b	F_d	F_s	$F_{i;1}$	$F_{i;2}$	$F_{dm;1}$	$F_{dm;2}$	F_u	F_r
TC1	1.2	0.25		1.0	1.0	1.0					1.0	
TC2	1.2	0.25		1.0	1.0		1.0				1.0	
TC3	1.2	0.25		1.0	1.0			1.0			1.0	
TC4	1.2	0.25		1.0	1.0				1.0		1.0	
TC5	1.2	0.25		1.0	1.0					1.0	1.0	
TC6	1.2	0.25		1.0							1.0	1.0
TC7	0.9			1.0	1.0	1.0					1.0	
TC8	0.9			1.0	1.0		1.0				1.0	
TC9	0.9			1.0	1.0			1.0			1.0	
TC10	0.9			1.0	1.0				1.0		1.0	
TC11	0.9			1.0	1.0					1.0	1.0	
TC12	0.9			1.0							1.0	1.0

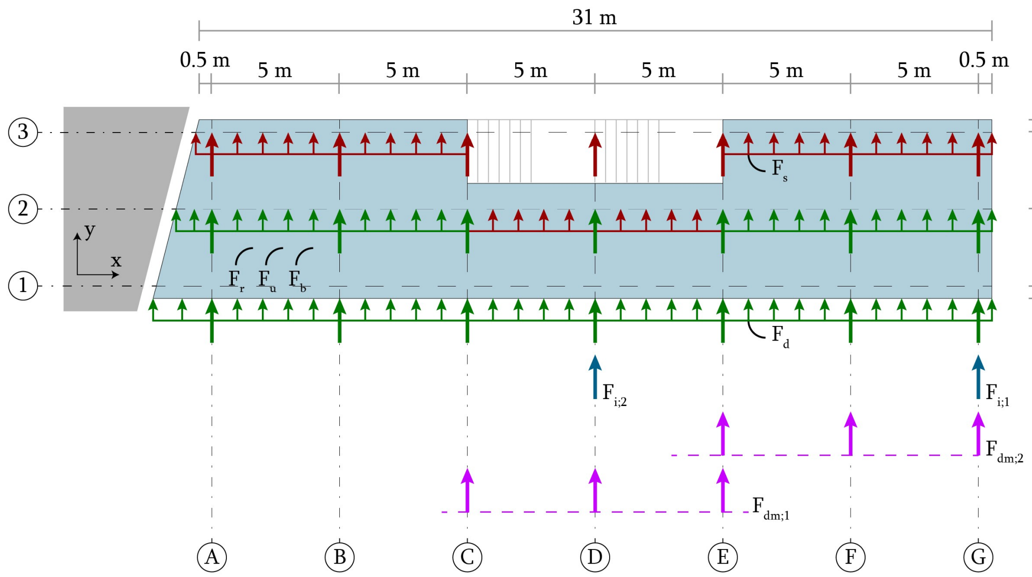

Figure 9-6: Configuration of tsunami loads

The different load combinations are analyzed with software ETABS. (ETABS, 2016) Unfortunately, the jetty will be severly damaged after the event of the tsunami. Most elements exceed the unity checks, as a result plastic deformations will occur and probably lots of elements will fail. As an example, after applying combination TC2 in ETABS including the debris impact force, the unity check of the pile at the corner exceeds 8.0, see Figure 9-7. In order to resist the impact force, the pile dimensions should be increased to a high extent, which is not feasible nor cost-effective for this relatively small design. It can be concluded that for this jetty it is not benificial to design against the impact of such a heavy tsunami.

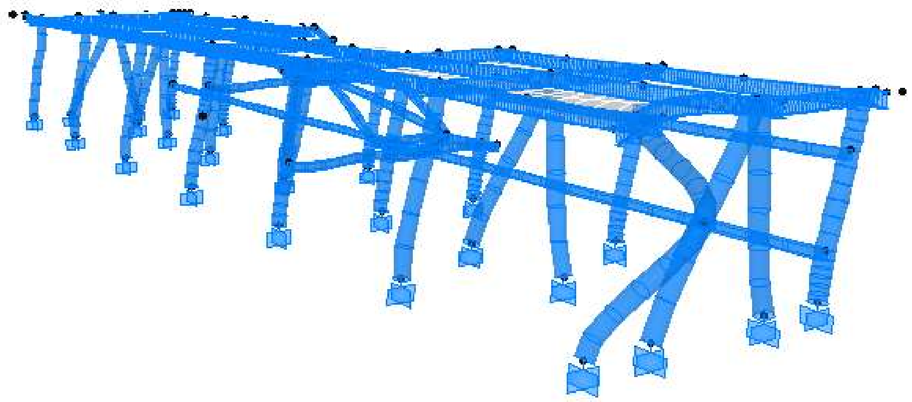

Figure 9-7: Deformation combination TC2

9.3.1.2 Geohazard: Scour

See chapter 6.2.7.2 Failure Mechanisms in 6.2.7: Final Design: Foundations for the treatment of scour around the jetty piles, which is assumed to not be of importance in the normal design case, due to the excavation of the layer of sediment. Here the steady current was assumed to be dominating. In the case of a tsunami event like that of Maule 2010, the wave may be governing. Due to large differences in scour properties between steady currents and tsunami waves, the tsunami-induced scour depth is a topic of much debate and current research, and an analytical method is lacking to date. However, Tonkin et al. suggest a limiting scour depth of 3m from post-tsunami field observations in Japan and Sumatra (2004). Thus, it is important to investigate the weatherability and susceptibility to scour erosion of the sedimentary bedrock to determine whether the jetty piles may be structurally affected by the theoretically proposed maximum scour depth. Mitigation measures in the form of quarry stone, gabions or matted aprons, or blankets, may have to applied around the piles.

9.3.2 BREAKWATER

9.3.2.1 Determining tsunami damage

In this part insight is gained in the effect of the tsunami on the breakwater. This part is meant to quantify, or at least to get an approximation of the damage caused by the tsunami. There are methods proposed for armour stability under tsunami attack, focusing on the current velocities (Kato, Suwa, Watanabe, & Hatogai, 2012). Though to determine the exact flow velocities at which the breakwater is exposed would take time consuming model calculations. These calculations are beyond the scope of this report. Therefor use is made of more general design formulae to get insight in the effects of the tsunami.

The authors of the Handbook of 'Coastal disaster mitigation for engineers and planners; advice to make use of the Hudson formula for the design of armour units in tsunami prone areas (Esteban, Takagi, & Shibayama, 2015). For a breakwater in a tsunami prone area, the armour units should first be designed using the Van der Meer or Hudson formula against wind waves in the area. This is the usual method in the design of any breakwater. Finally, at the end of the design procedure a check should be made that the breakwater meets the requirement of the formula adapted to tsunamis (Esteban, et al., 2013). The formula reads as follows:

$$W = A_t \frac{\gamma H_{tsunami}^3}{K_d (S_r - 1)^3 \cos \alpha} \tag{9.1}$$

W	$Required\ armor\ weight$	(ton)
A_t	$Coefficient\ depending\ on\ the\ structure\ type$	$(-)$
γ	$Desity\ of\ armor$	(ton/m^3)
$H_{tsunami}$	$Design\ wave\ heigth$	(m)
K_D	$damage\ coefficient$	$(-)$
s_r	$relative\ density\ armor$	$(-)$
α	$Slope\ of\ the\ structure$	$(°)$

To check if the design of the breakwater meets the requirements, the ratio: actual (designed) weight of the stones and the required weight of the stones to withstand tsunami impacts.

$$R = \frac{W_{actual}}{W_{required}} \tag{9.2}$$

However, the Hudson formula does not provide an indication of the degree of damage that can be expected due to a given event. Only an estimation can be made (Esteban, et al., 2013). The Van der Meer formula is used to try quantifying the damage of the breakwater. The Van der Meer Formula is formulated for plunging and surging waves, where a tsunami is a surging wave (bore type of wave) (Holthuijsen, 2007).

For plunging waves:

$$\frac{H_s}{\Delta D_{n50}} = \left(\frac{H_{2\%}}{H_s}\right)^{-1} 8.68P^{0.18}\left(\frac{bS}{\sqrt{N}}\right)^{0.2} \xi_m^{-0.5} \quad \text{if} \quad \xi_m < \xi_{mc} \tag{9.3}$$

For surging waves:

$$\frac{H_s}{\Delta D_{n50}} = \left(\frac{H_{2\%}}{H_s}\right)^{-1} 1.4P^{-0.13}\left(\frac{bS}{\sqrt{N}}\right)^{0.2} \sqrt{\cot\alpha_s}\,\xi_m^{p} \quad \text{if} \quad \xi_m > \xi_{mc}. \tag{9.4}$$

With the following parameters and limits:

Parameters:

M_{50}	*Armour unit mass*	(kg)
H_s	*Incident significant wave height*	(m)
T_m	*Mean wave period*	(s)
S	*Dimenssionles damage level*	$(-)$
ρ_a	*Armour density*	(kg/m^3)
ρ_w	*Water density*	(kg/m^3)
N	*Number of incoming waves*	$(-)$
P	*Notional permeability*	$(-)$
$H_{2\%}/H_s^*$	*Wave height ratio*	(kg/m^3)
A_e	*Erosion area*	(m^2)

Limits:

0.1	$\leq$	P	$\leq$	0.6
0.01 m	$<$	H_s	$<$	20 m
0.5 s	$<$	T_p	$<$	30 s
1.1	$<$	$\cot(\alpha_s)$	$<$	7.0
0.005	$\leq$	$2\pi H_s/gT_p^2$	$\leq$	0.06
0	$<$	N	$<$	7500
1.10	$<$	$H_{2\%}/H_s$	$<$	1.40
2000	$<$	ρ_a	$<$	3100 kg/m^3

S represents the dimensionless damage level: $S = \frac{A_e}{D_{n50}^2}$ (9.5)

The definition of the damage level is illustrated in Figure 9-8, the erosion area is the surface in a cross section that is displaced.

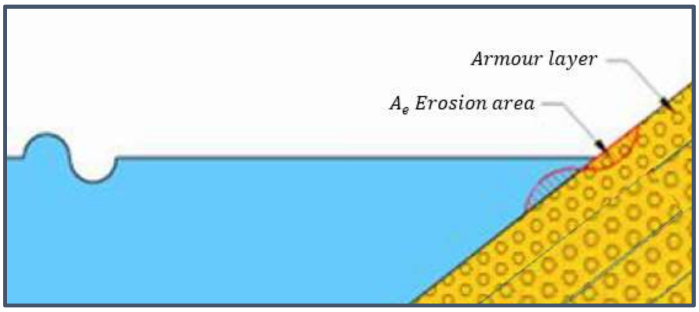

Figure 9-8: Illustration of breakwater damage level

The calculations with the Van der Meer formula are executed with BREAKWAT3.0. For an extensive explanation of BREAKWAT3.0, read Appendix H.3.

9.3.2.2 Input to compute tsunami damage

The modelled tsunami characteristics at this location (see also paragraph 9.3) are used as basis of the calculations. For the calculation of the required weight of armour units (W) with the Hudson formula, the following input in used:

Table 9-5: Input for Hudson formula

Parameter	Value	Unit	Source
$H_{tsunami}$	10.4	(m)	(Martinez & Aranguiz, 2016) (FEMA, 2011)
A_t	1	(-)	(Esteban, Takagi, & Shibayama, 2015)
γ	2650	(kg/m³)	(Schiereck & Verhagen, 2012)
K_D Trunk section	3.5	(-)	(Esteban, Takagi, & Shibayama, 2015)
K_D Round head	3	(-)	(Esteban, Takagi, & Shibayama, 2015)
S_r	1.5	(-)	(FEMA, 2011)
α	26.6	(°)	-

For the calculation to quantify the damage to the breakwater with the Van der Meer formula, the following input is used:

Table 9-6: Input for Van der Meer formula

Parameter	Value	Unit	Source
H_s	8	(m)	(Martinez & Aranguiz, 2016)
$H_{2\%}/H_s$	1.0	(-)	-
T_m	30	(s)	-
P	0.60	(-)	(Schiereck & Verhagen, 2012)
Cot(α)	2.0	(-)	-
N	20	(-)	-
M_{50}	10000	(kg)	-
ρ_w	1025	(kg/m³)	(FEMA, 2011)
ρ_a	2650	(kg/m³)	(Schiereck & Verhagen, 2012)

A value for $H_{2\%}/H_s = 1$ is chosen because in this case the value of H_s is also the maximum wave height. T_m is set on 30 seconds, which is the maximum wave period in the BREAKWAT design tool. The number of waves is set on 20 to ensure a conservative calculation. In reality the tsunami event contains around 10 big waves.

9.3.2.3 Output for tsunami damage

The calculation of the required weight of armour units (W) with the Hudson formula (9.1) gives the following results:

Table 9-7: Results from Hudson formula

Parameter	Trunk	Roundhead	Unit
$W_{required}$	10000	12000	(kg)
W_{design}	10000	10000	(kg)
R	1	0.83	(-)
$D_{n50\ required}$	1.56	1.65	(m)
$D_{n50\ Design}$	1.56	1.56	(m)

According to this values, there will not be damage at the trunk section of the breakwater. However, the roundhead of the breakwater will experience some damage. During a tsunami event, displacements of the elements located at the roundhead will occur. Because the Hudson formula does not provide an indication of the degree of damage that can be expected an estimation is made, using Figure 9-9.

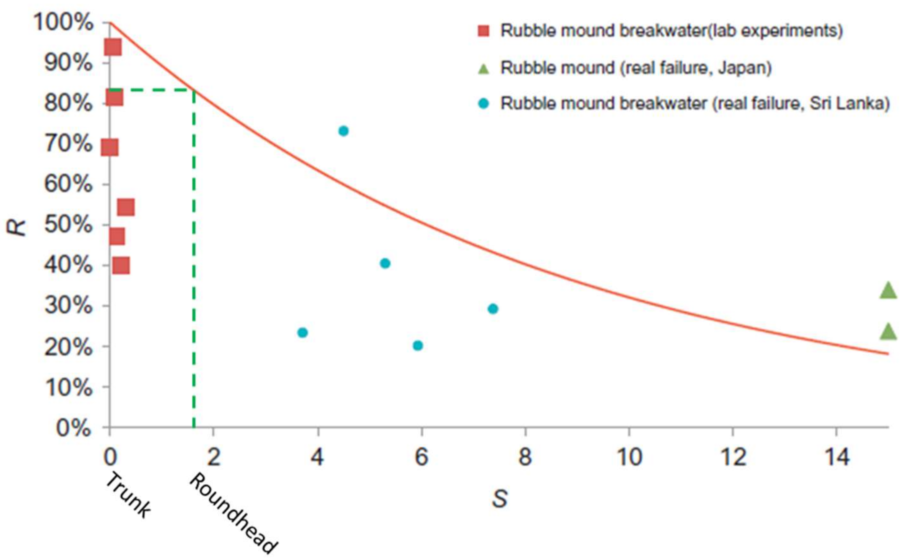

Figure 9-9: Estimate of damage level (Esteban, et al., 2013)

According to (Esteban, et al., 2013) value of the damage level at the roundhead of the breakwater can be estimated as S = 1.8. This damage level is equivalent to initial damage that needs to repaired. Nevertheless, no all-embracing rehabilitation is necessary.

The calculations made with the Van der Meer formula give a damage level of S = 0.3. The correctness of this value can be questioned. Basically, the Van der Meer formula is not conducted for tsunami waves. Hence, the tsunami characteristics are exceeding the limits for the Van der Meer formula. Moreover, the damage level is much lower than can be expected. Thereby the outcome of the calculation with the Van der Meer formula has no value.

Summarizing: The tsunami will cause damage to the breakwater. Because use is made of a very simple approximation, it is not possible to quantify the damage caused by the tsunami in detail. The degree of damage can be estimated on a damage level of S = 1.8. The breakwater is for this reason constructed out of just one stone dimension, to be able to recover it easily. A more comprehensive analysis is necessary to really quantify the movement of the stones. This study should consider currents instead of normal waves.

9.3.3 ONSHORE STRUCTURES

9.3.3.1 Geohazard: Scour

Building 11 in Figure 2-17 of Part I: Analysis is a critical onshore building, as it is the largest structure, is selected for redevelopment and it is located relatively close to the shore. Therefore, this building is considered for scour.

Scour could cause the soil underneath and between the footing to be removed, uplifting or tilting the structure, as observed elsewhere in Dichato during the Maule 2010 tsunami. Relationships exist describing tsunami induced scouring, such as that by Tonkin et al. (2003). However, data gathered for local scour depths induced by the 2011 Tohoku Tsunami in Japan (Tonkin, Francis, Bricker, & J.D., 2014) around structures suggest the following relationship between scour depth and flow depth

$$\begin{cases} d_{scour} & = 1.2H_{flow} \\ \max d_{scour} & = 3\ m \end{cases}$$

There is no apparent correlation of scour depth to soil type, possibly due to a very high Shield's parameter. An added effect to tsunami induced scour is that of liquefaction due to rapid drawdown, which from the data seemed the dominating contributor to scouring around structures (Tonkin, Francis, Bricker, & J.D., 2014).

In the case of EMBD building 11, the maximum flow depth H_{flow} here was 7m during the Maule 2010 event. This would give a scour depth which would be limited by the maximum of 3m, which is indeed realistic in this case as the geophysical test has delineated the presence of rock at 3m below ground surface.

Mitigation measures include placing the top of the foundation slab below the scour depth of 3m. This is unrealistically deep and not cost-effective for a shallow foundation slab. Short piles may be a better foundation option to avoid scour effects, but given the lack of application of deep foundations for low-rise buildings in Chile this is unlikely to be implemented, either.

9.3.3.2 Geohazard: Slope failure

Tsunamis have in past seismic events triggered major landslides in the Concepcion area, see Appendix K for more theory behind slope failures and past event in the area. During site visits it was observed that several slopes behind the Marine Biology Station at Punta Villarrica showed evidence of past failures in the form of debris at the toe and exposed slide surfaces. A slope along profile I-I' in Fig K-4 in Appendix K1 is situated right behind the Marine Biology Station and presents a possible hazard to the Station. If the slope were to fail in its entirety, it could impact the road running along structures at the EMBD site.

A slope stability rating system, Hack's Slope Stability Probability Classification, is used to analyse both the mass and local instability of the slope in question. The SSPC is a three-step classification system based on the probabilistic assessment of independent failure mechanisms as a result of field records of the slope.

An outcrop of the slope under consideration under consideration is shown in Figures K-2 and K3 in Appendix K.1. The rock in question is soft sandstone from the Curanilahue formation, with thin to thick bedding and two other identified discontinuity sets. Thin slabs of the rock break easily in the hand. For a filled out SSPC-form, see Appendix K.1.

The SSPC results are as follows: in terms of global failure the slope is highly unstable (<5% probability of stability), see Figure 9-10. This is caused by the low intact rock strength of the material. In terms of discontinuity-dependent instability, the bedding plane is only 5% stable, whilst joint set 1 is highly stable at >95% probability of stability. Figure 9-11 indicates that joint set 3 is unstable but in fact its apparent dip coincides with the slope dip and therefore the probability of sliding failure is low.

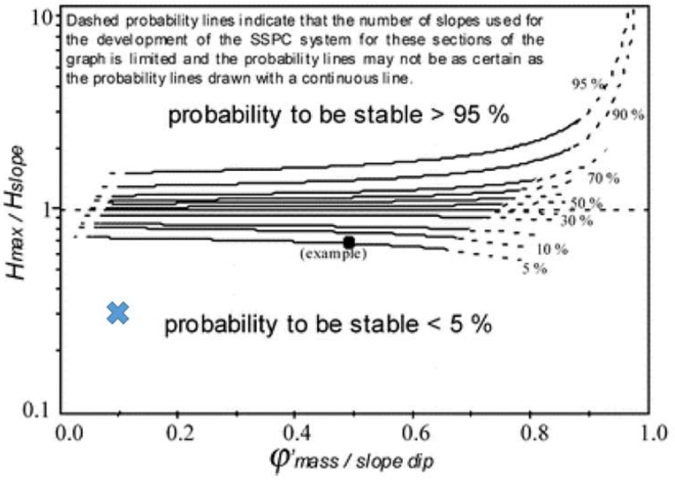

Figure 9-10: Orientation-independent failure -probability of mass failure of the slope (Hack, 2003)

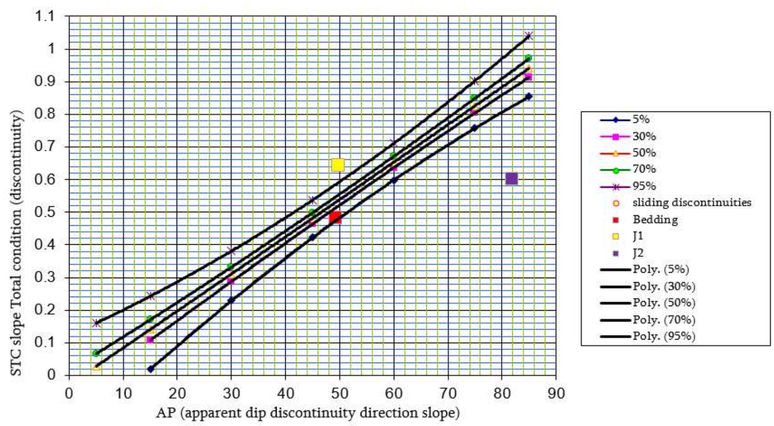

Figure 9-11: Orientationy-dependent failure -probability of sliding failure for each discontinuity set

9.4 SUMMARY OF RISKS AND MITIGATION

9.4.1 JETTY

Failure mechanism	Natural event	Risk (=probability x consequence)	Mitigation measures
Collapse due to high lateral displacements	Earthquake	Low, structure designed for lateral seismic loads	Design with appropriate safety factors
Pile-short effect	Earthquake	Low because all piles have same length	Maintain dredged water depth
Liquefaction-induced differential settlement, or bending and buckling of piles	Earthquake	Low due to the excavated overlying sand	Maintain dredged water depth; low slope angle; and avoid build-up of loose sediment
Foundation scour	Tsunami	Low due to the excavated overlying sand	Maintain dredged water depth and avoid build-up of loose sediment
Pounding from adjacent structure (abutment)	Earthquake	Low, enough space in between two structures guaranteed	Ensure and maintain enough space in between structures

9.4.2 BREAKWATER

Failure mechanism	Natural event	Risk (=probability x consequence)	Mitigation measures
Global instability	Earthquake / Tsunami	Low	None
Settlement crest	Earthquake	Low probability and easy to rehabilitate consequence.	None, rehabilitation afterwards, if necessary.
Slope deformation	Earthquake	Low in comparison to tsunami.	None, rehabilitation afterwards, if necessary.
Individual stone displacement	Tsunami	Probable when extreme impact occurs, with as major consequence the hitting of the jetty piles.	Heavy stones (W_{50} 10.000 kg)

9.4.3 ONSHORE STRUCTURES

Failure mechanism	Natural event	Risk (=probability x consequence)	Mitigation measures
Structural failure	Earthquake / tsunami	Low consequences: building is constructed to be resilient	Ensure resilience and rehabilitation capacity: all primary functions in top floor.
Liquefaction and lateral spreading	Earthquake	Top 3m of sand are susceptible to liquefaction, high risk of unallowable settlement.	Dynamic compaction of sand.
Foundation scour	Tsunami	High level of uncertainty in tsunami-induced scour depth prediction	Place top of foundation at least 3m below ground surface.
Slope failure	Tsunami	High probability of mass failure / debris flow of slope behind EMBD, could affect major part of scope area.	Drainage measures on slope; prevent toe erosion by tsunami through added support; and ensure resilience in structures which could be affected.

10 CONSTRUCTION PROCESS

10.1 DREDGING

The breakwater and jetty have been designed according to certain water depth and subsurface conditions, which must be established before construction of either of these two elements. Therefore, after the accessibility of the site is ensured, a first step of this project is the dredging of soft soils and some rock removal at the locations of the breakwater and the jetty. The sand layer on top of the sedimentary rock may be removed by backhoe on a pontoon, whilst the removal of weathered top layer of sandstone may be carried out with a cutter tool. The depth contours before and after the dredging are shown in Figure 10-1 and Figure 10-2.

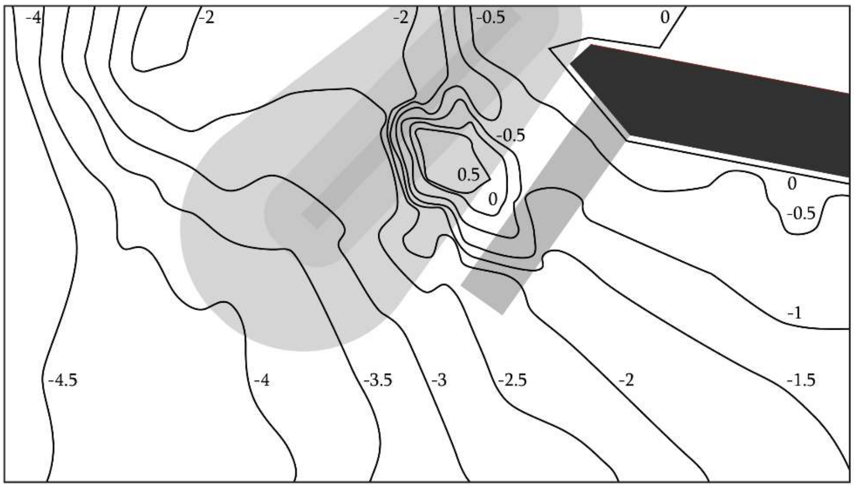

Figure 10-1: Depth contours before dredging

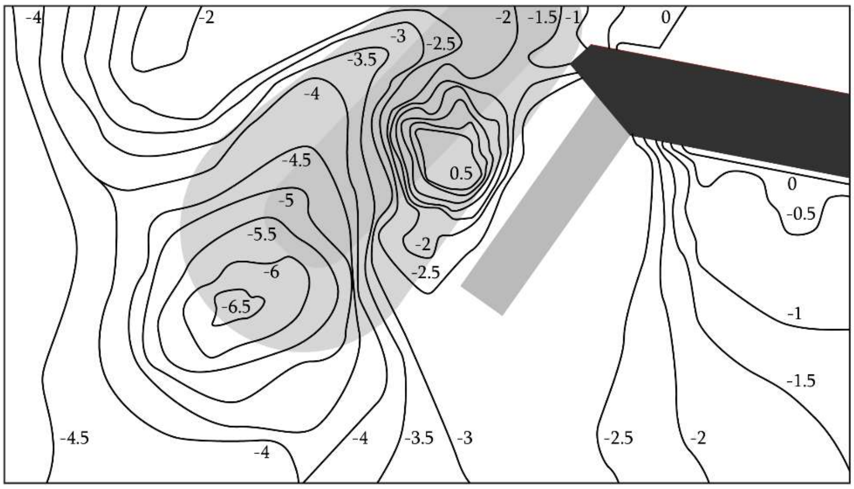

Figure 10-2: Depth contours after dredging

10.2 CONSTRUCTION TIMELINE

Figure 10-3 shows a rough timeline for the construction of the various elements part of the EBMD design proposal. Note that because prior to construction, a license and funding must be granted by the local Department of Port Works, and these aspects are not included in the time planning in the figure. Therefore, the start time of actual construction is uncertain.

The critical path (in orange) shows the main dependencies and the resulting total construction time, which is estimated at 35 weeks. The optimal time of the year to construct is after August, since storms before this time could hinder the construction of the breakwater. It is also important to finish construction before the summer holidays in February, which would otherwise interrupt work for at least a month.

In theory, the construction of the breakwater, the redevelopment of the building onshore and the placement of the pavement can start simultaneously as soon as site preparation has been carried out. The construction of the jetty may commence as soon as the breakwater has been placed and has ensured calm waters.

Some main uncertainties in the planning lie in the dredging works around the jetty and the pile driving, due to inherent unknowns in subsurface conditions, and relative inexperience with dredging involving some rock removal. There are also many uncertainties in the redevelopment of the building. It is unknown to what extent the current concrete frame is structurally sound and problems with the concrete, reinforcement or foundation slab may only be discovered upon stripping.

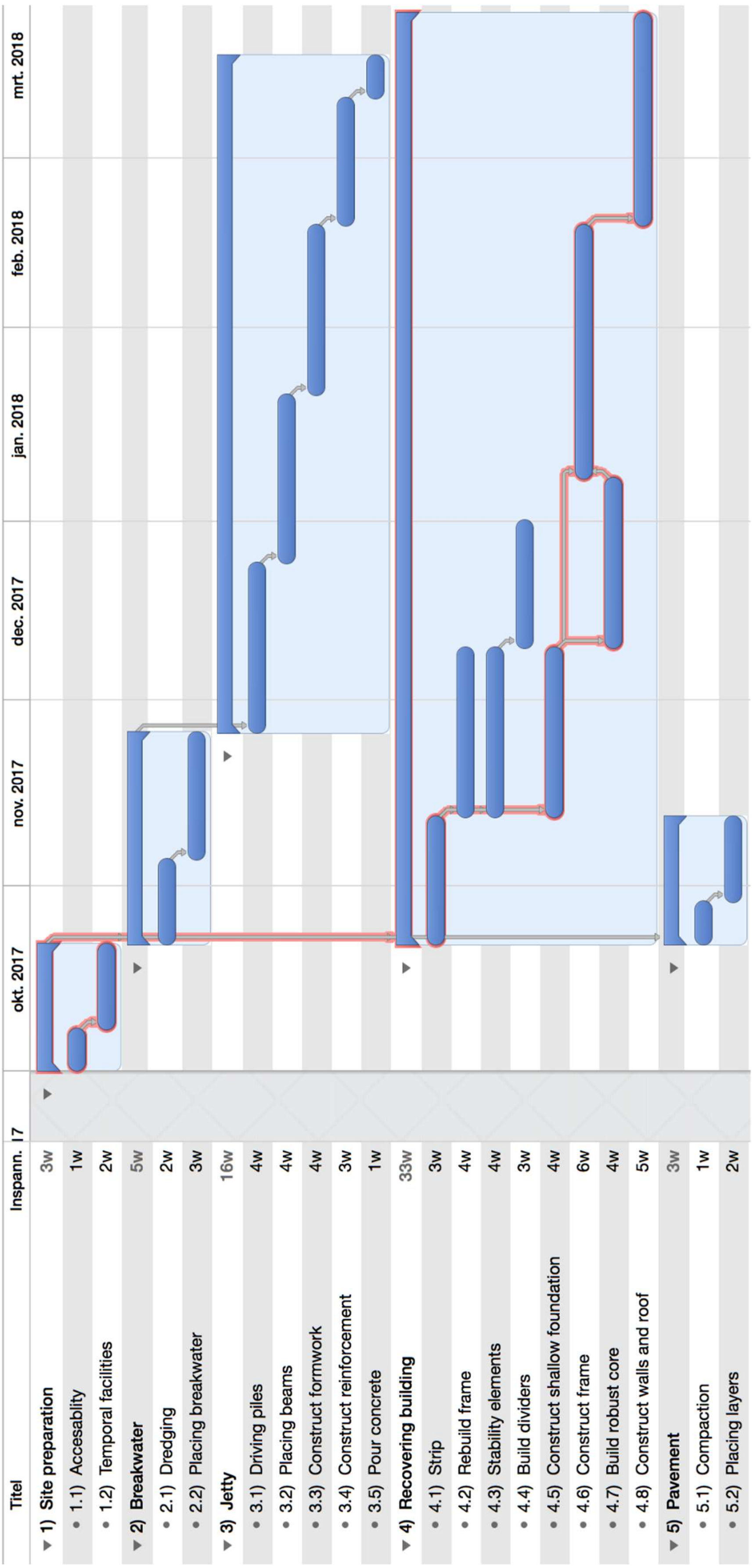

Figure 10-3: Project construction timeline

11 Cost Breakdown

A more detailed cost breakdown, including general preparatory work and the construction of the pavement and redeveloped building are given in Table 11-1. For source of prices please consult Chapter 4.2 of Part I: Analysis.

Table 11-1: Cost breakdown of design proposal

	Number	Unit	Unit price (CLP)		Costs (CLP)		Costs (EUR)	
Site preparation					$	6,200,000	€	8,986
Dredging works					$	15,750,000	€	22,826
GENERAL					**$**	**21,950,000**	**€**	**31,812**
Vertical piles	17	no.	$	362,498	$	6,162,473	€	8,931
Inclined piles	4	no.	$	386,665	$	1,546,660	€	2,242
Pile driving	21	no.	$	475,000	$	9,975,000	€	14,457
Pile anchoring	4	no.	$	10,000,000	$	40,000,000	€	57,971
Beams purchase	16	no.	$	362,498	$	5,799,974	€	8,406
Beams placing (5 men + crane)	5	days	$	2,100,000	$	10,500,000	€	15,217
Construction formwork deck	198	m2	$	6,699	$	1,326,402	€	1,922
Reinforcement deck	0.45	m3	$	4,056,000	$	1,825,200	€	2,645
Concrete deck	45	m3	$	80,000	$	3,600,000	€	5,217
Purchase installations	1	-	$	4,000,000	$	4,000,000	€	5,797
Placing installations (5men)	5	days	$	100,000	$	500,000	€	725
Crane purchase (1000kg)	1	no.	$	1,380,000	$	1,380,000	€	2,000
Placing Crane (2 men + crane)	1	days	$	2,040,000	$	2,040,000	€	2,957
Purchase steel mooring stairs	1	no.	$	14,000,000	$	14,000,000	€	20,290
Placing stairs (7 men + crane)	3	days	$	2,140,000	$	6,420,000	€	9,304
JETTY					**$**	**109,075,709**	**€**	**158,081**
Armour stones and placement	4600	m3	$	20,000	$	92,000,000	€	133,333
BREAKWATER					**$**	**92,000,000**	**€**	**133,333**
Stripping and construction	720	m2	$	120,000.00	$	86,400,000.00	€	125,217
REDEVELOPED BUILDING					**$**	**86,400,000.00**	**€**	**125,217**
Waste material from armourstone quarrying	57.6	m3	$	6,342	$	365,299	**€**	**529**
Crushed Concreet (process)	43.2	m3	$	2,600	$	112,320	**€**	**163**
Microsurface	18	m3	$	6,000	$	108,000	**€**	**157**
Machinery and labour	118.8	m3	$	6,549	$	778,021	**€**	**1,128**
PAVEMENT					**$**	**1,363,640**	**€**	**1,976**
SUBTOTAL					**$**	**310,789,349**	**€**	**450,419**
Unforeseen costs 20% of sub-total					$	62,157,870	**€**	**90,084**
Maintenance 1% of sub-total per year	25	years	$	3,107,893	$	77,697,337	**€**	**112,605**
TOTAL					**$**	**450,644,557**	**€**	**653,108**

12 CONCLUSIONS AND RECOMMENDATIONS

12.1 CONCLUSIONS

- Currently the EBMD of UdeC cannot perform its main objectives of scientific and academic research in a safe and efficient manner, especially since the destruction following Maule 2010. A jetty is proposed as a mooring facility, in combination with a breakwater to protect it and the EBMD vessel from waves, which are determined to be relatively high in this part of Coliumo Bay.
- A 'Traditional' jetty design is proposed with steel piles in a Marco Duplas configuration in order to provide a suitable structural period to cope with seismic loading (i.e. not too flexible to avoid large deformations, and not too rigid in order keep the design slender). The concrete deck rests on steel beams. All elements are dimensioned to be structurally sound.
- The construction of a breakwater in the front of a jetty protects the jetty and the moored vessel from wave impact under normal design wave conditions. However, it does not protect the jetty during a tsunami event. The breakwater consists of armour stones of median diameter 1.56m and median weight 10.000 kg.
- Neither the breakwater or the jetty are likely to suffer severe damage during a large-scale earthquake event. The ensuing tsunami, however, may cause damage to the round-head of the breakwater, but this damage is repairable with the existing stones. Debris impact may cause extensive deformations of parts of the jetty.
- The EBMD as a whole is upgraded through the redevelopment of a building which is designed with resilience in mind as a tsunami mitigation method currently very popular in Chile. Also, the upgrade of the pavement using a surface protection layer prevents the necessity of regular maintenance and solves on-site dust emission problems.
- Dredging must be carried out prior to construction to remove the soft soils overlying the sedimentary rock. These soils are susceptible to liquefaction during an earthquake, and associated lateral spreading and scouring. In the design of both the jetty and the breakwater it is assumed that the structures rest on bedrock.
- The construction is estimated to take around 35 weeks and ought to be carried out preferably between the months of October and May. The costs associated with the construction of the various elements of the design as well as a 25-year maintenance period are estimated at 450 mil CLP or 650,000 EUR. This estimation of construction time and costs does not include preliminary site investigation, planning or obtainment of permits.

12.2 Recommendations

The following recommendations include considerations that ought to be made for a next design phase; some draw-backs of the current design; and missing information which would aid a final decision on the feasibility of the design proposal.

Overall, to attract funding for the project from the Department of Port Works of the Bío-Bío region, a further design phase may involve the widening of the scope to include more stakeholders. If the concrete abutment were able to be used by artisanal fishers, or an enlargement of the jetty would be considered, an integration between UdeC and inhabitants of Dichato could stimulate government and university interest.

12.2.1 Jetty

- In order to develop the final design of the jetty, the current preliminary design should be investigated in more detail. Considered loads can be calculated more precisely and more load configurations can be researched. For example, the influence of impact loads on other elements of the structure can be analysed.
- All structural joints have to be analysed and calculated more thoroughly. Detailed drawings have to be created which will explain the type, principle and dimensions of the connections. The connection between the concrete abutment and the jetty needs special attention, as up to this point only the basic principle has been explained.
- For the current preliminary design, the frame of the staircase and the defence beams including its rubber defenders are assumed to be similar to the ones from the Bachelor Thesis (Sandoval Munoz, 2010). In the final design, these frames and the defenders need to be studied more extensively.
- For the extreme impact evaluation the influence of the Maule earthquake needs to be analysed. This will require in a dynamic analysis including the whole spectrum of the earthquake, resulting in certain displacements and damaging of the structure.
- The impact of the subsequent tsunami of 2010 could be researched in more detail by using the output from the aforementioned dynamic earthquake analysis as input before adding the tsunami loads.
- The current solution to prevent uplift of the piles subject to tension (inclined) is to anchor them into the rock using a micropile. However, this may not be the optimal solution. It must be investigated whether it is more economical to simply take pile with a larger diameter and embed it deeper into the sedimentary rock without anchorage. This will depend on the required diameter needed to obtain sufficient weight and skin friction to resist pull-out, and associated steel cost.
- The assumption was made that the existing concrete abutment is undamaged and has a high structural resistance. However, this needs to be researched in more detail through several analysis methods: non-destructive methods (e.g. visual assessment, Impact-Echo (IE), Surface Penetrating Radar (SPR)) and/or destructive methods (e.g. coring, cutting, drilling) (Grill, 2011).

12.2.2 BREAKWATER

- For a final design of the breakwater a more in detail design needs to be elaborated. The focus of this project was rather on defining the wave climate in the bay of Coliumo than on the design of the breakwater. Investigation into the optimization of the slope, crest width and damage level can be done. Moreover, a consideration can be made to make use of a berm, core and toe structure.
- The construction process of the breakwater is not elaborated in this report. Associated with the optimization of the breakwater for a final design, also a construction plan can be determined. Both a detailed design and an execution plan of the construction needs to be included in the construction plan.
- In the final design, also a more in depth investigation into the effect of the tsunami waves is of importance. In the current damage evaluation use is made of more general formulas to estimate the damage to the breakwater caused by the tsunami. To really quantify the movement of the stones, a detailed study into the flow velocities around the stones is required. With this information also a better founded determination of distance between the breakwater and jetty can be made.
- Improvements of the study into the wave climate in the bay of Coliumo are possible. The Delft3D-WAVE model can be improved by accounting for the 30 cm water level increase by low air pressure during a North Western storm (Winkler et al. 2016) and some model related improvements can be made.
- A study can be made to the sediment transport around the breakwater and jetty. The soil will be excavated here and hence, the sediment balance is disturbed. This might result in problems regarding maintenance dredging and additional scouring/ accumulation.

12.2.3 FOUNDATIONS AND GEOHAZARDS

- In general, site investigation, in the form of SPTs and boreholes must be carried at a more relevant location. In this design, use was made of six SPTs conducted in 2010, four of which were performed further offshore than relevant for the location of the jetty and breakwater and hence may not accurately reflect the current subsurface conditions at the location of choice.
- It has been assumed in the design of the jetty and breakwater that both rest on sedimentary bedrock, since the 1-2m of overlying sands are dredged away prior to construction. However, in the long run, sediments may accumulate once again and present various hazards to foundation stability. Sediment transport, especially behind the breakwater, warrants more investigation.
- To investigate scour at both the jetty piles and at the breakwater more accurately, the weatherability or susceptibility to scour erosion of the sedimentary bedrock must be analysed. In the preceding analysis it has been assumed that the bedrock is not susceptible to erosion at all, but since it concerns soft rock, this may not reflect the true conditions.
- Only a single slope analysis was conducted near the EBMD, even though the area had many unstable slopes. A more complete survey of slopes ought to be made, and a coherent slope stabilization scheme for the hills behind the coastline may be established.

12.2.4 EBMD Building

- The EBMD building selected for redevelopment must be analysed structurally in a next design phase, as up until here only a conceptual design has been made. Dimensioning the structural elements will also give a better idea of costs and the corresponding feasibility of the construction of this tsunami-resilient building. Perhaps it is more profitable to design the building as the other buildings on site have been redeveloped since 2010 (two floors with no separate structures).

12.2.5 Pavement

- It is likely not feasible to use recycled concrete as sub-base material for the pavement. Although often applied in The Netherlands, the in Chile rarely carried out process of concrete cleaning and preparation would render this solution more expensive than obtaining crushed rock from nearby quarries.
- In the case of future expansion of the EBMD facilities, or merging with other functionalities such as artisanal fishing, the capacity of the on-site infrastructure must be re-evaluated. It may be of use to compare (in a MCA) various pavement options which may be suitable for more intense use, such as asphaltic solutions or thin concrete slabs.

References

AASHTO, L. (1998). *Bridge design specifications.*

ACI Committee 318. (2008, January). Building Code Requirements for Structural Concrete (ACI 318-08) and Commentary. American Concrete Institute.

ANSI. (2005). *AISC 360-05-Specification for Structural Steel Buildings.* Chicago: AISC.

Awad, A., & Ayoub, A. (1976). Ultimate uplift capacity of vertical and inclined piles in cohesionless soil. *Proceedings of the 5th international conference on soil mechanics and foundation engineering, Budapest.*

Baeriswyl, S. (2015). Nuevos desafíos urbanos y nuevas herramientas de planificación. Urbano 9.

Breusers, H. N., Nicollet, G., & Shen, H. W. (1977). Local scour around cylindrical piers. *Journal of Hydraulic Research 15.3*, 211-252.

Broms, B. (1964). Lateral resistance of piles in cohesive soils. *Journal of the Soil Mechanics and Foundation Division*, 27-64.

Bustos, A. (2016, December 22). Lecture on Seismically Isolated Structures. UdeC, Concepcion.

Canam Group. (2016). *Seismic Isolators: GOODCO Z-TECH.* Quebec.

Crane Authority. (2009). *Crane Authority.* Retrieved 2009, from http://www.craneauthority.com/

Esteban, M., Jayaratne, R., Mikami, T., Morikubo, I., Shibayama, T., Danh Thao, N., . . . Ohtani, A. (2013). Stability of breakwater armour units against tsunami. *J. Waterw. Ports Coast. Ocean Eng.*, 188–198.

Esteban, M., Takagi, H., & Shibayama, T. (2015). *Handbook of Coastal disaster mitigation for engineers and planners.* Oxford UK: Elsevier.

ETABS. (2016, 12 19). ETABS (2016) [Software]. Retrieved from https://www.csiamerica.com/products/etabs#

FEMA. (2008). *Guidelines for Design of Structures forVertical Evacuation fromTsunamis .* NOAA, FEMA. California: FEMA.

FEMA. (2011). *Coastal Construction Manual P-55; Principles and Practices of Planning, Siting, Designing, Constructing, and Maintaining Residential Buildings in Coastal Areas (Fourth Edition).* FEMA, Washington.

Grill, J. M. (2011). Assessment of Existing Concrete Structures in the Absence of Drawings. Whitlock Dalrymple Poston & Associates, PC.

Guzmán A., F. (2010). Norma Chilena Oficial Nch3171.Of2010. *Diseño estructural - Disposiciones generales y combinaciones de cargas*. Instituto Nacional de Normalización.

Hack, R. (2003). A new approach to rock slope stability–a probability classification (SSPC). *Bulletin of Engineering Geology and the Environment 62.2*, 167-184.

Haigh, S. K. (2000). Lateral spreading during centrifuge model earthquakes. *ISRM International Symposium.* International Society for Rock Mechanics.

Hidalgo, O. P. (1986). Norma Chilena Oficial Nch1537.Of86. *Diseño estructural de edificios - Cargas permanentes y sobrecargas de uso*. Instituto Nacional de Normalización.

Hidalgo, O. P. (1996). Norma Chilena Oficial NCh433.Of1996. *Diseño sísmico de edificios*. Instituto Nacional de Normalización.

Hidalgo, O. P. (2003). Norma Chilena Oficial Nch2369.Of2003. *Diseño sísmico de estructuras e instalaciones industriales*. Santiago, Chile: Instituto Nacional de Normalización.

Hidalgo, O. P. (2010). Norma Chilena Oficial NCh3171.Of2010. *Diseño estructural - Disposiciones generales y combinaciones de cargas*. Santiago, Chile: Instituto Nacional de Normalización.

Holthuijsen, L. (2007). *Waves in oceanic and coastal waters.* TU Delft and UNESCO-IHE. Cambridge: Cambridge.

Ibáñez V., J. (1971). Norma Chilena Oficial Nch432.Of71. *Cálculo de la acción del viento sobre las construcciones*. Instituto Nacional de Investigaciones Tecnológicas y Normalización.

ICA. (2000). Manual de Diseno para Estructuras de Acero. Instituto Chileno del Acero.

IIASA. (2015, December 2). *International Centre for Geohazards (ICG).* Retrieved from International Institute for Applied Systems Analysis: http://www.iiasa.ac.at/web/home/research/ResearchPartners/International-Centre-for-Geohazards.en.html

Instituto Chileno del Acero. (2000). Manual de diseño para estructuras de acero. *Metodo de factores de carga y resistencia*. Instituto Chileno del Acero S.A.

Instituto Chileno del Acero. (2000). Manual de diseño para estructuras de acero. Instituto Chileno del Acero.

Kato, F., Suwa, Y., Watanabe, K., & Hatogai, S. (2012). *Mechanismof coastal dike failure induced by the Great East Japan Earthquake Tsunami.* Santander, Spain: In: Proc. of 33rd Int. Conf. on Coastal Engineering.

Martinez, C., & Aranguiz, R. (2016). Riesgo de tsunami y planificacion resiliente de la costa chilena. *Revista de Geogradia Norte Grane*, 33-54.

Memos, C., Bouckovalas, G., & Tsiachris, A. (2012, 04 26). Stability of rubble mound breakwaters under seismic action. *Coastal engineering*.

Nave, R. (n.d.). *Simple harmonic motion*. Retrieved 12 26, 2016, from HyperPhysics: http://hyperphysics.phy-astr.gsu.edu/hbase/shm.html

NNI. (2006). *NEN 6740:2006 Geotechnics -TGB 1990 - Basic requirements and loads.* Delft: Nederlands Normalisatie-instituut.

OCDI . (2009). *Technical standards and commentaries for port and harbour facilities in Japan.* Overseas Coastal Area Development Institute of Japan.

PDCA. (2001). Recommended design specifications for driven bearing piles. Pile Driving Contractors Association.

Poulos, H. (2006). Raked piles - Virtues and drawbacks. *Journal of geotechnical and geoenvironmental engineering 132.6*, 795-803.

SAFE. (2016). SAFE (2016) [Software].

Sandoval Munoz, C. A. (2010). *Diseno del Atracadero para la Estacion Biologia Marine en Dichato.* Concepcion: Universidad de Concepcion.

Schiereck, G., & Verhagen, H. (2012). *Introduction to bed, bank and shore protection.* Delft: VSSD.

Srinivasamurthy, B. R., & Pujar, K. L. (2009). Socketing of bored piles in rock. *Proceedings of Indian Geotechnical Conference.* Guntur.

Steel Flooring Products Co. (n.d.). *Straight flight staircases.* Retrieved 12 19, 2016, from Steel Flooring Products: http://www.steelflooring.ie/index.html

Thenoux, G., & al, e. (2002). *Guía de diseño estructural de pavimentos para caminos de bajo volumen de tránsito.* Dirección de Vialidad, Ministerio de Obras Públicas de Chile.

Tol, A. (2006). *CTB1410(67) Funderingstechnieken.* Delft, The Netherlands: Delft University of Technology.

Tonkin, A., Yeh, H., & Heller, E. (2004). Mechanisms of scour induced by tsunami runup. *Proceedings of the 2nd international conference on scour and erosion*, (p. Vol. 2). Singapore.

Tonkin, S. P., Francis, M., Bricker, & J.D. (2014). Limits on Coastal Scour Depths due to Tsunami. *International Efforts in Lifeline Earthquake Engineering*, 671-678.

TU Eindhoven. (n.d.). Vuistregels voor globale dimensionering.

Verhagen, H. J., d'Angremond, K., & van Roode, F. (2009). *Breakwaters and closure dams.* TU Delft. Delft: VSSD.

Wang, H., Yang, C. Y., Lamison, C., & Chen, S. S. (1978). *Loadings on rubble-mound breakwaters due to earthquakes.* University of Delaware. Delaware: Coastal Engineering.

Wijdeven, B. (2015). *Marinas and cruise terminals (Ports and Waterways 2).* Presentatie, TU Delft , Hydraulic engineering, Delft.

Yang, X., & Jin, X. (2015, 02 11). Dynamic analysis of a rubble-mound breakwater subject to earthquake including seawater–structure-foundation interaction. *Journal of Engineering for the Maritime Environment*(230), 310-326.

Yasuda, S., Verdugo, R., & Konagai, K. (2010). Case History: Geotechnical damage caused by the 2010 Maule, Chile earthquake. *ISSMGE Bulletin: Volume 4, Issue 2*, 16-27.

Youd, T., Idriss, I., Andrus, R., & Arango, I. (2001). "Liquefaction resistance of soils: summary report from the 1996 NCEER and 1998 NCEER/NSF workshops on evaluation of liquefaction resistance of soils. *Journal of geotechnical and geoenvironmental engineering 127.10*, 817-833.